(1) 690 400
(4) $5.00

(1)

FIRST SEMI-ANNUAL PROGRESS REPORT

For the Period

1 October 1962 - 31 March 1963

STUDIES OF THE FUNDAMENTAL CHEMISTRY PROPERTIES AND BEHAVIOR OF FUEL CELLS

Submitted to:

National Aeronautics and Space Administration

NsG 325

(11) 31 March 63

(12) 55p

(13) NA

14- 1/1 NA

11

NA

Submitted by

Professor J. O'M. Bockris, Director

The Electrochemistry Laboratory

The University of Pennsylvania

Philadelphia 4, Pennsylvania

TABLE OF CONTENTS

POTENTIALS OF ZERO CHARGE

I. Introduction

The most important reference point in all studies on adsorption is the point of zero charge of metals. This is obtained easily for liquid metals by electrocapillary measurements. However, for solid electrodes, the most valuable methods are: A: The study of adsorption of organic substances in dilute solutions by means of capacity measurements by means of an a.c. method; and B: Adsorption studies by radioactive methods. Development of the first method is under study.

II. Experimental

A. At the beginning, many factors had to be examined to ensure the applicability of the method.

1. The cell was constructed so that the high purity techniques used generally in this laboratory can be applied. (It has often been stated that this is not necessary for a dropping electrode, but even here the parallel resistance of the double layer impedance was shown to be affected by impurities; and on solid electrodes, the effects are very marked.)

The solutions are purified by pre-electrolysis and recrystallization and/or distillation. Purified hydrogen is bubbled through the system which is kept free from oxygen (air). The temperature is kept constant to better than $\pm$ 0.1°C because both solution resistance and capacitance of the double layer vary strongly with temperature.

2. The impedance bridge used in the present set-up is not a Wheatstone bridge (such as the bridges used before, e.g., by Grahame, Melik-Gaikazyan, and others) but a transformer ratio arm bridge

(Wayne-Kerr B221). The equivalent circuit in the bridge is arranged in parallel, since it is assumed that this arrangement corresponds to the model of the double layer.[1]

The standards and the unknown impedance are compared through precision-wound transformers; therefore a small number of standards (only 2 conductance and 2 capacitance standards) of higher impedance are used. This reduces appreciably false variations of capacitance and resistance with frequency as observed with Wheatstone bridges. The signal applied is only 5 mV and can be reduced further (without a significant effect on accuracy) to about 1/2 mV. To reach this result it was necessary to shield and ground the entire set-up carefully; and in the detector circuit, a wave analyzer of narrow band width was used as selective amplifier. The frequency is constantly checked with a counter so that accurate determinations can be made at a range of frequencies (the readings of conductance and capacitance are in a parallel equivalent circuit; a conversion to a corresponding series equivalent circuit must be made which involves the value of the frequency used).

3. In the circuit the polarizing and the potential measuring branches are connected to the test electrode-reference electrode system in such a way that the measuring a.c. signal is practically only applied to the system studied, and no false frequency variation or errors are introduced by their presence. The test electrode and the counter electrode (for application of the small a.c. signal from the bridge) are arranged spherically symmetrically; with KCl and HCl solutions of various concentrations it was ascertained that the resistance of the

solution showed the expected variation with concentration and no variation with frequency. The double layer capacitance as checked on the dropping electrode also was shown not to vary with frequency; this is considered to be a test for the bridge methods. For the normal measurements, frequencies between 1 and 5 kcps are used in order to get the most accurate results. The bridge has been tested between 160 and 16000 cps.

The potential of the test electrodes can be measured with respect to reference electrodes which are reversible to the anion or cation, respectively, of the electrolyte (cf. thermodynamic methods for the surface excess from the values of the differential capacity measured).

These values, obtained as a function of potential, are fed with a suitable program in a computer to obtain an equation for a polynomial curve fit:

$$C = a + bV + cV^2 + dV^3 + \ldots$$

where C = capacitance (in $\mu F\ cm^{-2}$), V = potential vs. a reference electrode (in millivolts), a, b, c, d, etc., are constants. This equation is readily integrated, and the values of the charge density on the electrode:

$$q = \int C dV$$

and of the surface tension for the Hg electrode used for the testing of the method:

$$\gamma = - \int q dV$$

are calculated. They are compared to electrocapillary data obtained in our Laboratory. The surface tension values obtained in this way are used to derive the surface excess of ions and molecules adsorbed at the

interface:

$$\Gamma = -\frac{d\gamma}{d\mu}$$

(where Γ = the Gibbs surface excess, μ the chemical potential), and these are again compared (for H^+ and Cl^- in HCl solutions) with electrocapillary results. Adsorption data from capacitance measurements will be directly compared to adsorption data from electrocapillary measurements to prove thermodynamically their validity.

Results obtain as yet with the Hg electrode in HCl and KCl solution have proved that the described electronic circuit is appropriate to the model of the solution electrode interface and is suitable to carry out capacitance measurements with an accuracy of about 0.1%.

B. Adsorption of naphthalene and ethylene on gold and platinum was studied.

1. The method used[2] consisted in determination in situ of the surface excess of the adsorbate under potential control in a closed system by means of radioactive measurement. The radiations from the labeled adsorbate pass through the metal foil (20,000 Å thick) into the Geiger-Muller flow-counter. The efficiency of the counter and the count-rate originating from solution are determined by calibration[2] with standard solution of $Na_2CO_3^{14}$, thus permitting evaluation of the absolute value of the amount adsorbed.

2. A standard technique for obtaining reproducible Pt surfaces by platinizing gold foils was developed (sufficiently thin Pt foils without pinholes are not available).

3. Gold foils were rinsed consecutively with acetone and distilled water, and pulsed anodically for 10 sec at a current density .107 amp/cm^2, in 1 N H_2SO_4 solution. Then the electrode was lifted to remove bubbles and pulsed again for 10 sec anodically at .107 amp/cm^2. Bubbles are removed again and electrode remains in the solution for 20 min., and is then cathodically pulsed for 30 secs. The first 10 sec. the current density is increased up to .107 amp/cm^2 and is continued at that density for the remainder of the 30 secs. The solution is then replaced by a fresh solution of 1 N H_2SO_4 and the electrode is pulsed cathodically again for 30 sec with the first 10 sec used to reach .107 amp/cm^2.

The gold foil was cleaned and then platinized with current density 6.6×10^{-3} A/cm^2 for 3 minutes. The platinizing solution consists of 3 grams of chloroplatinic acid dissolved in 100 grams of conductivity water. A bright platinum surface is obtained. In order to achieve reproducibility, it was found that the cleaning technique of the platinum surface is critical. The surface is bathed in concentrated sulfuric acid for 20 minutes and is then pulsed alternately (in 1 N H_2SO_4) anodically then cathodically for 3 seconds and 7 seconds respectively ten times at a current of 6.6×10^{-3} amp/cm^2 with final cathodic pulse lasting 30 seconds.

Apparatus used in the quoted papers was modified in that the part exposed to the atmosphere in the closed system containing the electrode and the electrolytic cell was redesigned and made of Teflon to prevent possible impurities and corrosion products to enter the system.

The technique of working with the gaseous adsorbates had been improved in that the concentration of the dissolved gas may be independently measured by the measurement of pressure and volumes, and also by coulometric titration with bromine.[3]

4.a. Adsorption of naphthalene on platinum

Adsorption occurs between + 0.100 - + 1.100 V (N.H.E.) showing no potential dependence in this range. Outside those limits sharp desorption takes place. The process is irreversible in that the electrode exposed to potentials above + 1 V, do not adsorb any naphthalene more even at lower potentials (oxide formation).

b. Adsorption of ethylene on gold.

No conclusive results have as yet obtained. The apparent lack of potential dependence (Fig. 1) may be due to the too low concentrations of ethylene used.

c. Adsorption of ethylene on platinum.

Adsorption of ethylene on Pt (Fig. 2) shows a definite potential dependence with the maximum in the vicinity of (+ 0.7 V). The results cannot be yet calculated in terms of the fractional coverage, since the roughness factor of the platinized surface had not yet been determined. The same irreversibility as in the case of naphthalene adsorption on Pt was found.

References

1. J. O'M. Bockris and B. Conway, J. Chem. Phys., 28, 707, 1958.

2. H. Wroblowa and M. Green, Electrochimica Acta (in press).

   H. Dahms and M. Green, Nature, Vol. 196, No. 4861, pp. 1310-1311 December 29, 1962.

   H. Dahms and J. Weber, Nature, 1311, 1962.

3. F. A. Leisey, J. F. Grutach, Anal. Chem. 28, 1553 (1956).

   R. J. Meyers, E. H. Swift, J. Am. Chem. Soc., 70, 1047 (1948).

9x10⁻⁵ MOLAR ETHYLENE ON GOLD

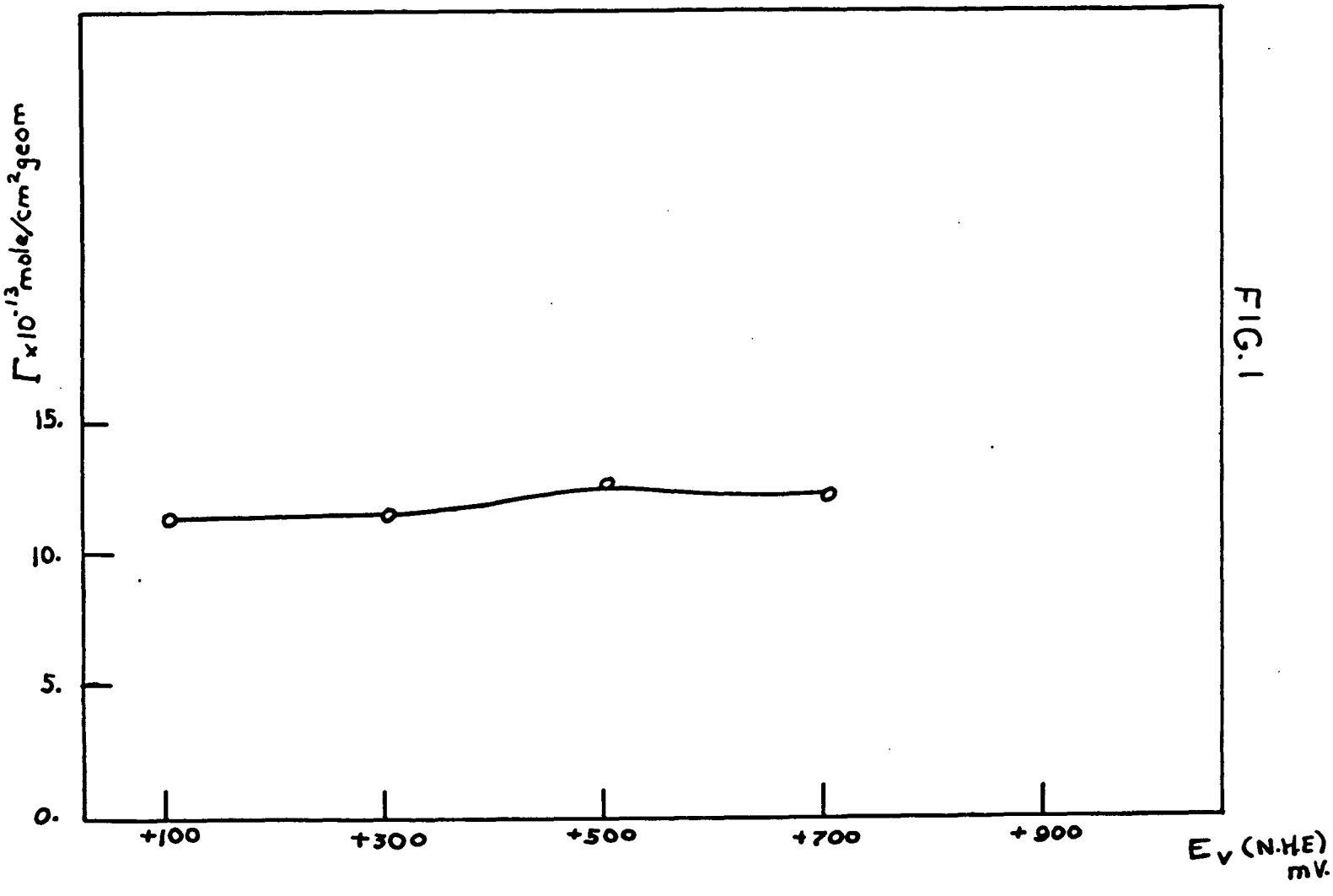

FIG. 1

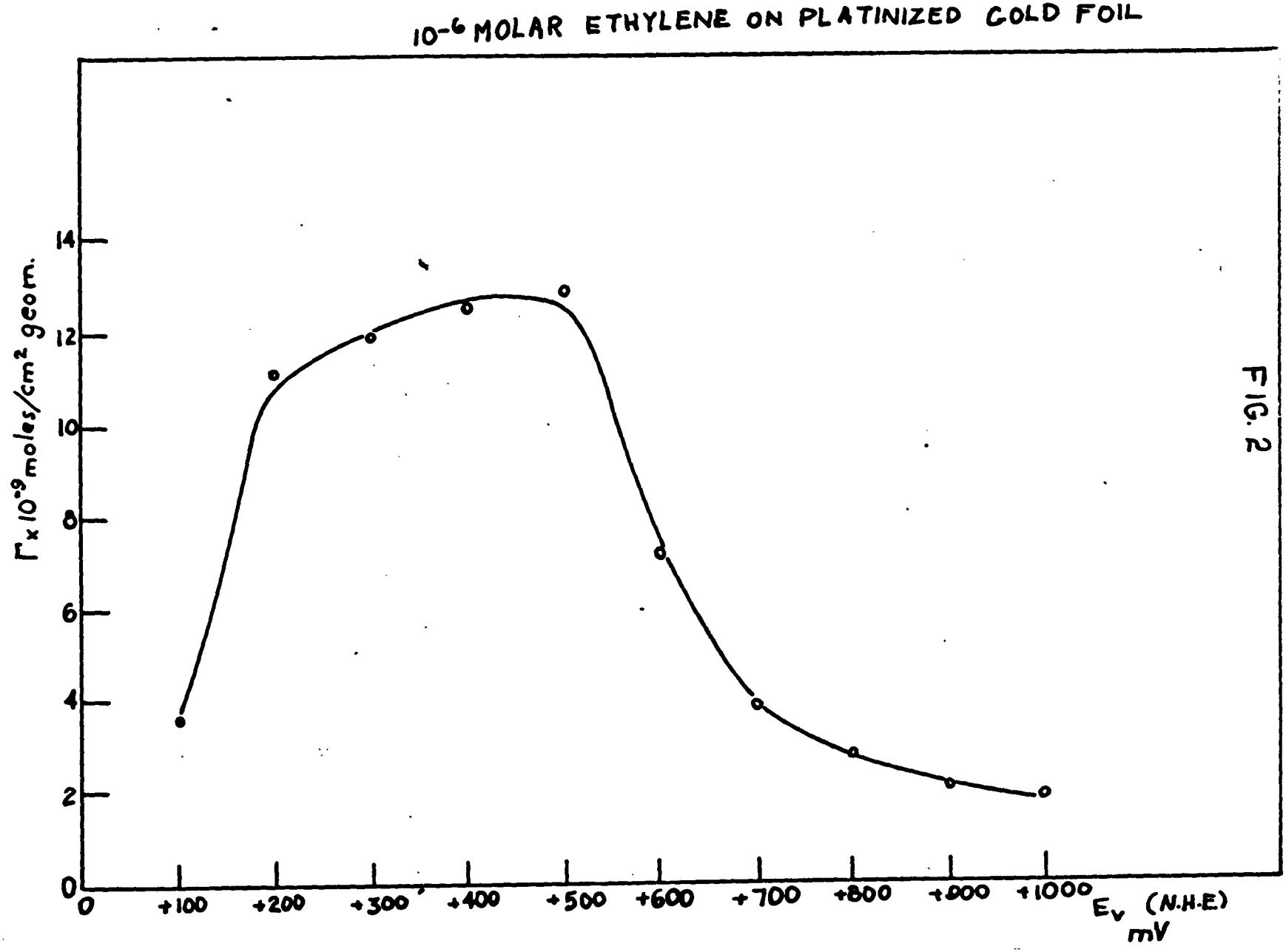
10-6 MOLAR ETHYLENE ON PLATINIZED GOLD FOIL
Γ x 10-9 moles/cm2 geom.
14
12
10
8
6
4
2
0
0
+100
+200
+300
+400
+500
+600
+700
+800
+900
+1000
Ev (N.H.E.) mV

FIG. 2

DEACTIVATION OF CATALYSTS: ADSORPTION

I. Introduction

Little information is available on the adsorption of organic compounds from aqueous solution on solid metal electrodes. This is in part due to the experimental difficulty of obtaining such data, since measurements of the surface tension or the capacity, which yield data for the adsorption on mercury cannot be made sufficiently accurate on solids. A knowledge of the adsorption behavior of organic compounds is of great importance in electrode kinetics since the rate of a reaction may be increased or decreased many times by the presence of an adsorbed layer. In particular, deactivation of an electrode is often due to the adsorption of impurities on the active sites.

II. Experimental

a. The Tape Method. The present method consists of adsorbing C-14 labeled organic materials on an electrode in the form of a tape, which is drawn through the electrolyte bath. The tape is left stationary in the electrolyte containing the tagged organic material for a sufficiently long time to reach equilibrium and is then withdrawn in such a way that the layer of solution adhering to the tape is only about one micron thick. The total activity on the tape is then measured and the background from the adhering solution is subtracted. The thickness of the liquid layer was measured by placing metal plates on either side of the tape and measuring the capacity between them and the tape first with the liquid film on the tape and then with the tape dry. Knowing the concentration of the active material in solution, the amount of radioactive

material present, the film could be calculated. This background correction is a small one, typically 5% - 10%, whereas in previous methods using radioactive tracers the background from the solution was generally larger than the radiation from the adsorbed material. In addition, since the radiation is not measured through the metal the need for extremely thin foils is eliminated. The tapes used were 0.5" wide by 0.002" thick. These dimensions are determined by considerations of strength and flexibility of the tapes. Iron, nickel and copper tapes of these dimensions were used. Lead and platinum were also investigated but a lead tape of these dimensions would not have sufficient tensile strength while a platinum tape would be too costly. In these cases the metals were clad onto a nickel base, i.e. a thin layer of Pb or Pt was rolled onto both sides of the base metal to give a compound tape of the same size as that given above.

b. Results. The adsorption of naphthalene and n-decylamine on the 5 metals mentioned above was measured as a function of the concentration of the organic in solution and as a function of the electrode potential. The potential range varied for the different metals. The limits are hydrogen bubble formation on the cathodic side since bubbles on the electrode interfere with the attainment of the adsorption equilibrium. On the anodic side dissolution of the metal or oxide formation is the limit. Results are shown in the attached figures. Knowing the amount of organic adsorbed and the actual surface area of the tapes (from B.E.T. surface area measurements) the coverage (θ) was calculated.

III. Conclusions

The following general features of the adsorption process on solid metals have been observed.

1. In the potential range available in acid solutions n-decylamine adsorbs only to a very small extent ($\theta < 8\%$) from a 10^{-4} molar solution, while adsorptions approaching a monolayer occur from alkaline solutions.

The same is true for the adsorption of naphthalene except in the case of platinum where a complete adsorption curve could be measured in acid solution, as well as in alkaline solution.

2. The adsorption maximum in general occurs at a potential several hundred millivolts cathodic of the present estimate of the zero charge potential in the absence of the organic molecule. For Pt the adsorption maximum coincides with the zero charge potential in the absence of organic.

3. The relationship between the potential of maximum adsorption and coverage is not a simple one. Positive, negative and zero shifts of the maximum with coverage have all been observed.

4. Both linear and Langmuir type isotherms (not shown in this report) have been observed.

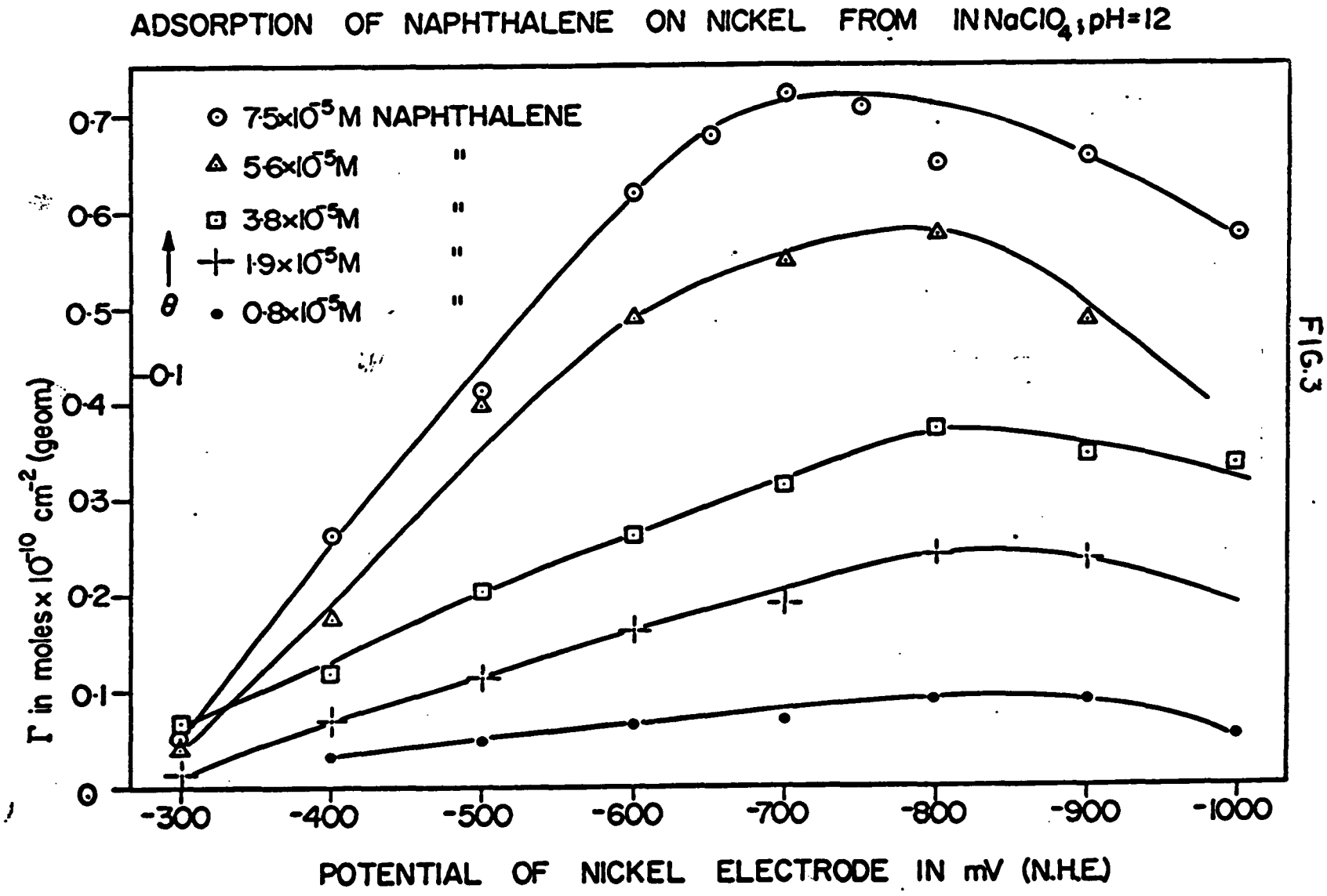
ADSORPTION OF NAPHTHALENE ON NICKEL FROM IN NaClO4 ; pH=12
⊙ 7·5×10⁻⁵M NAPHTHALENE
△ 5·6×10⁻⁵M "
⊡ 3·8×10⁻⁵M "
+ 1·9×10⁻⁵M "
• 0·8×10⁻⁵M "
θ
0·7
0·6
0·5
0·1
0·4
0·3
0·2
0·1
0
Γ in moles × 10⁻¹⁰ cm⁻² (geom)
-300
-400
-500
-600
-700
-800
-900
-1000
POTENTIAL OF NICKEL ELECTRODE IN mV (N.H.E)

FIG.3

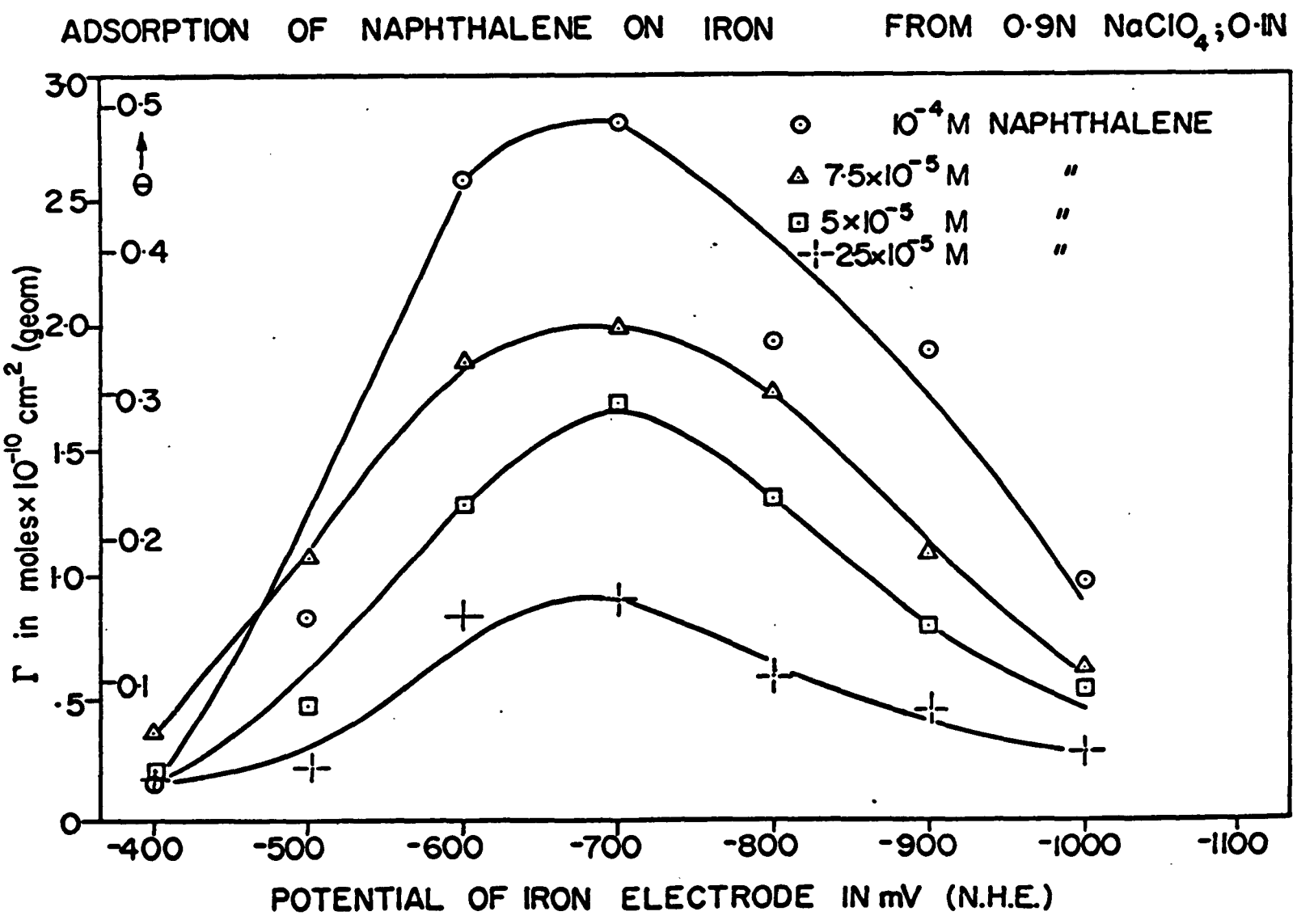
ADSORPTION OF NAPHTHALENE ON IRON FROM 0·9N NaClO4 ; 0·1N NaOH
10⁻⁴M NAPHTHALENE
7·5×10⁻⁵M "
5×10⁻⁵ M "
2·5×10⁻⁵ M "
θ
Γ in moles×10⁻¹⁰ cm⁻² (geom)
POTENTIAL OF IRON ELECTRODE IN mV (N.H.E.)
0·5
0·4
0·3
0·2
0·1
3·0
2·5
2·0
1·5
1·0
·5
0
-400
-500
-600
-700
-800
-900
-1000
-1100

FIG.4

ADSORPTION OF NAPHTHALENE ON COPPER FROM IN $NaClO_4$

FIG.5

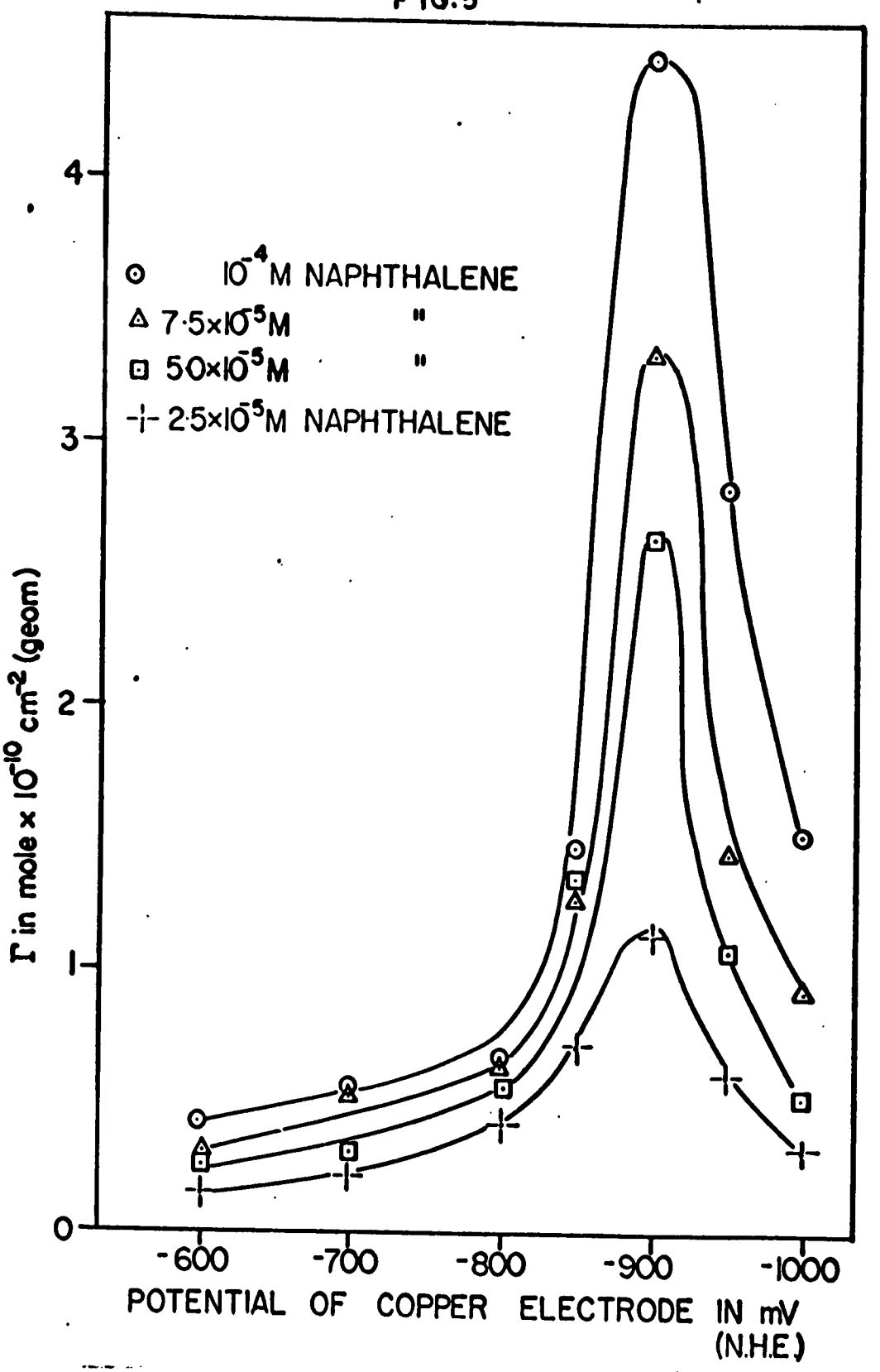

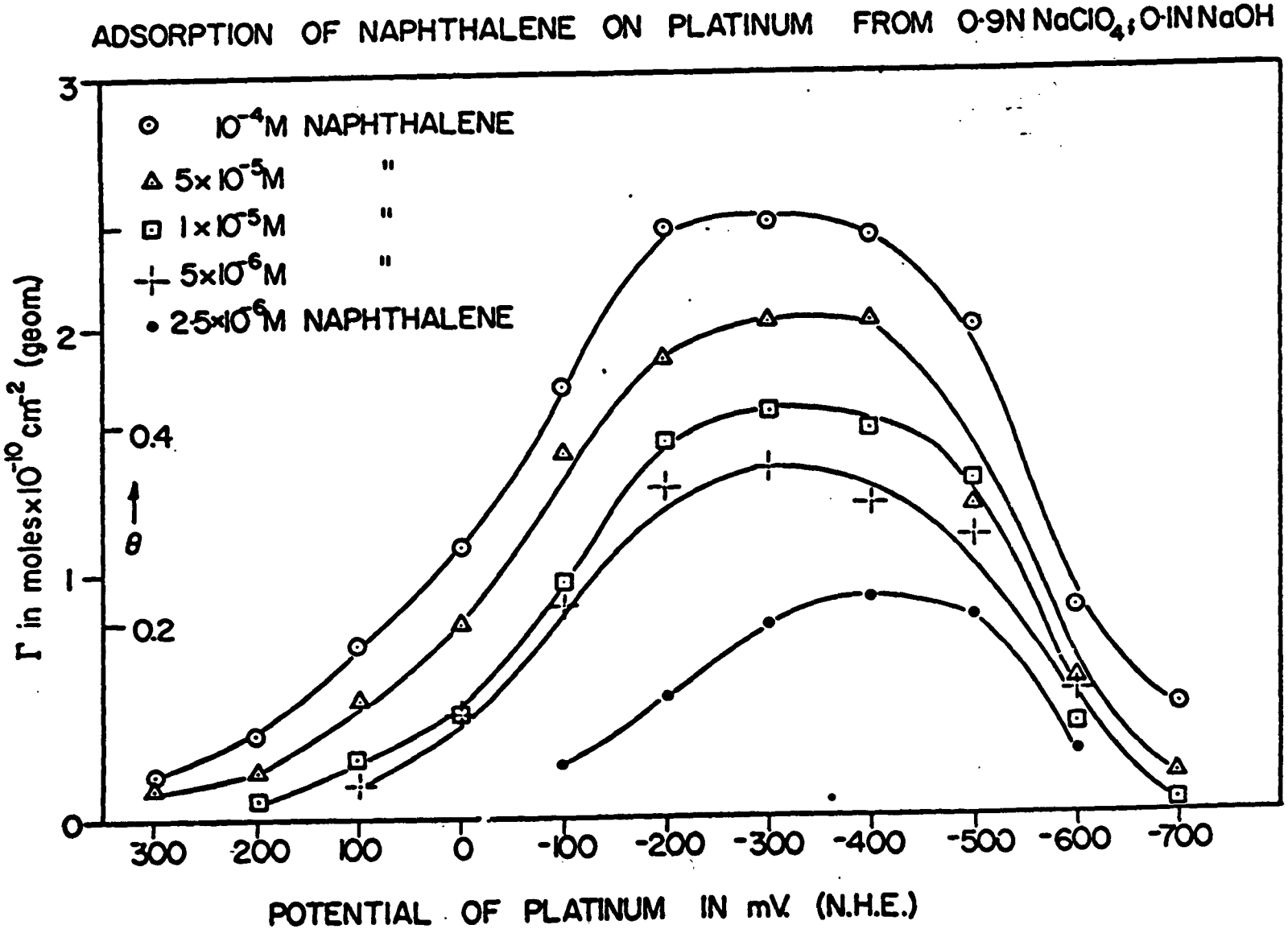
ADSORPTION OF NAPHTHALENE ON PLATINUM FROM 0·9N NaClO4; 0·1N NaOH
10⁻⁴M NAPHTHALENE
5×10⁻⁵M "
1×10⁻⁵M "
5×10⁻⁶M "
2·5×10⁻⁶M NAPHTHALENE
Γ in moles×10⁻¹⁰ cm⁻² (geom)
θ
0.4
0.2
3
2
1
0
300
200
100
0
-100
-200
-300
-400
-500
-600
-700
POTENTIAL OF PLATINUM IN mV. (N.H.E.)

FIG. 6

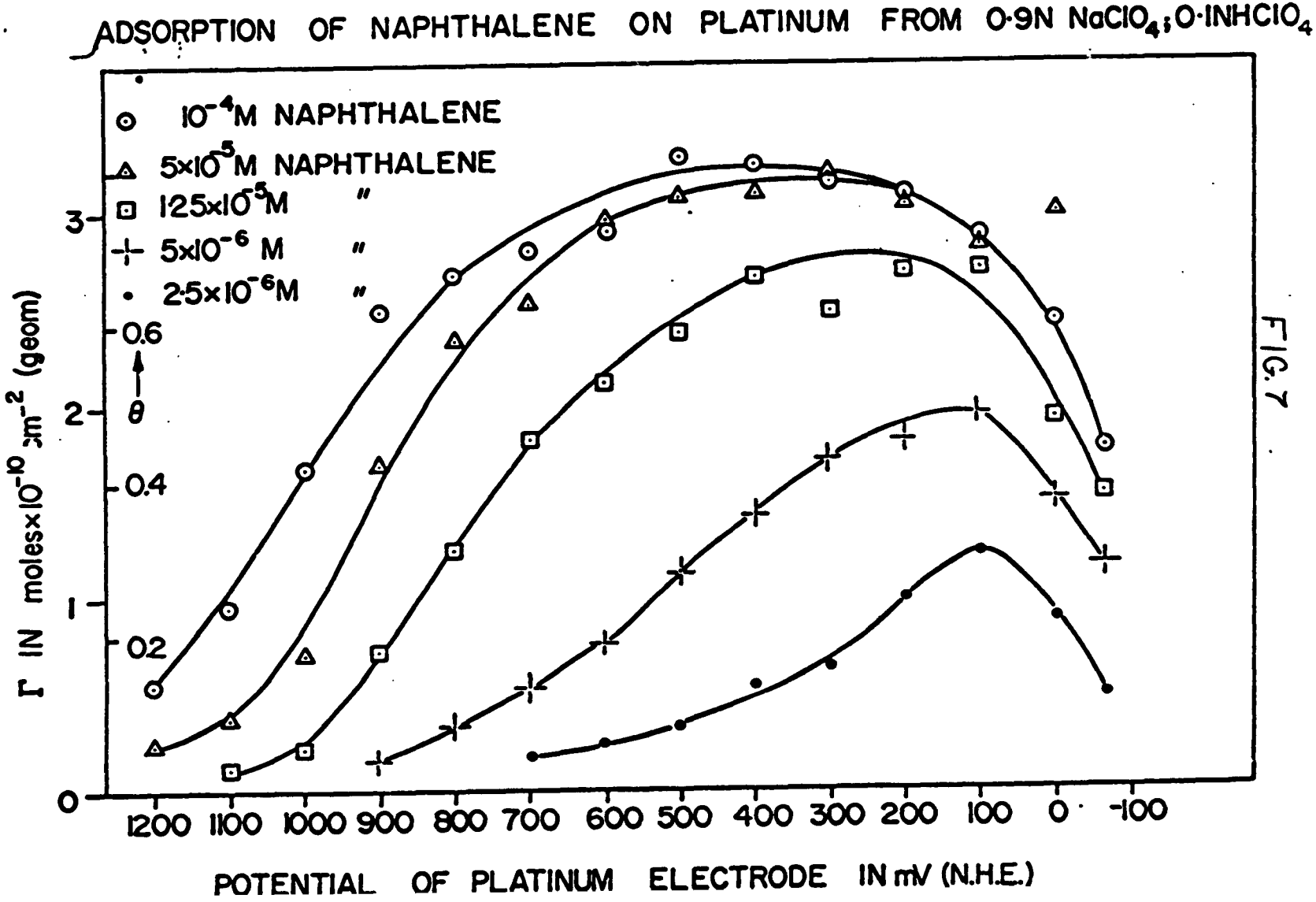
ADSORPTION OF NAPHTHALENE ON PLATINUM FROM 0·9N $NaClO_4$; 0·1N $HClO_4$
10^{-4}M NAPHTHALENE
5×10^{-5}M NAPHTHALENE
1.25×10^{-5}M "
5×10^{-6} M "
2.5×10^{-6}M "
θ
0.6
0.4
0.2
Γ IN moles$\times10^{-10}$ cm^{-2} (geom)
0
1
2
3
1200 1100 1000 900 800 700 600 500 400 300 200 100 0 -100
POTENTIAL OF PLATINUM ELECTRODE IN mV (N.H.E.)

FIG. 7

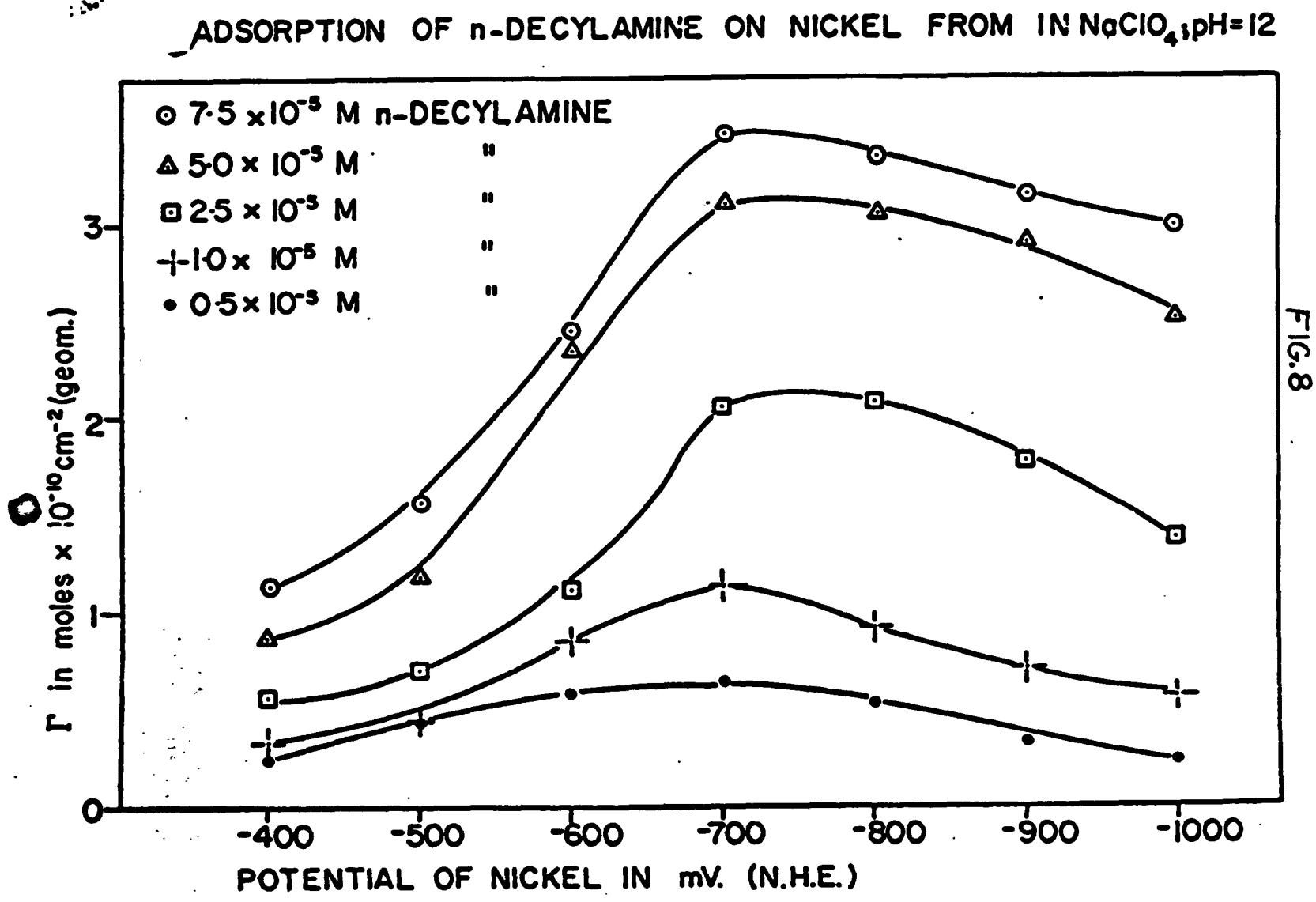
ADSORPTION OF n-DECYLAMINE ON NICKEL FROM 1N NaClO4 pH=12
⊙ 7·5 x10⁻⁵ M n-DECYLAMINE
△ 5·0 x 10⁻⁵ M "
⊡ 2·5 x 10⁻⁵ M "
+ 1·0 x 10⁻⁵ M "
• 0·5 x 10⁻⁵ M "
Γ in moles x 10⁻¹⁰ cm⁻² (geom.)
0
1
2
3
-400
-500
-600
-700
-800
-900
-1000
POTENTIAL OF NICKEL IN mV. (N.H.E.)

FIG. 8

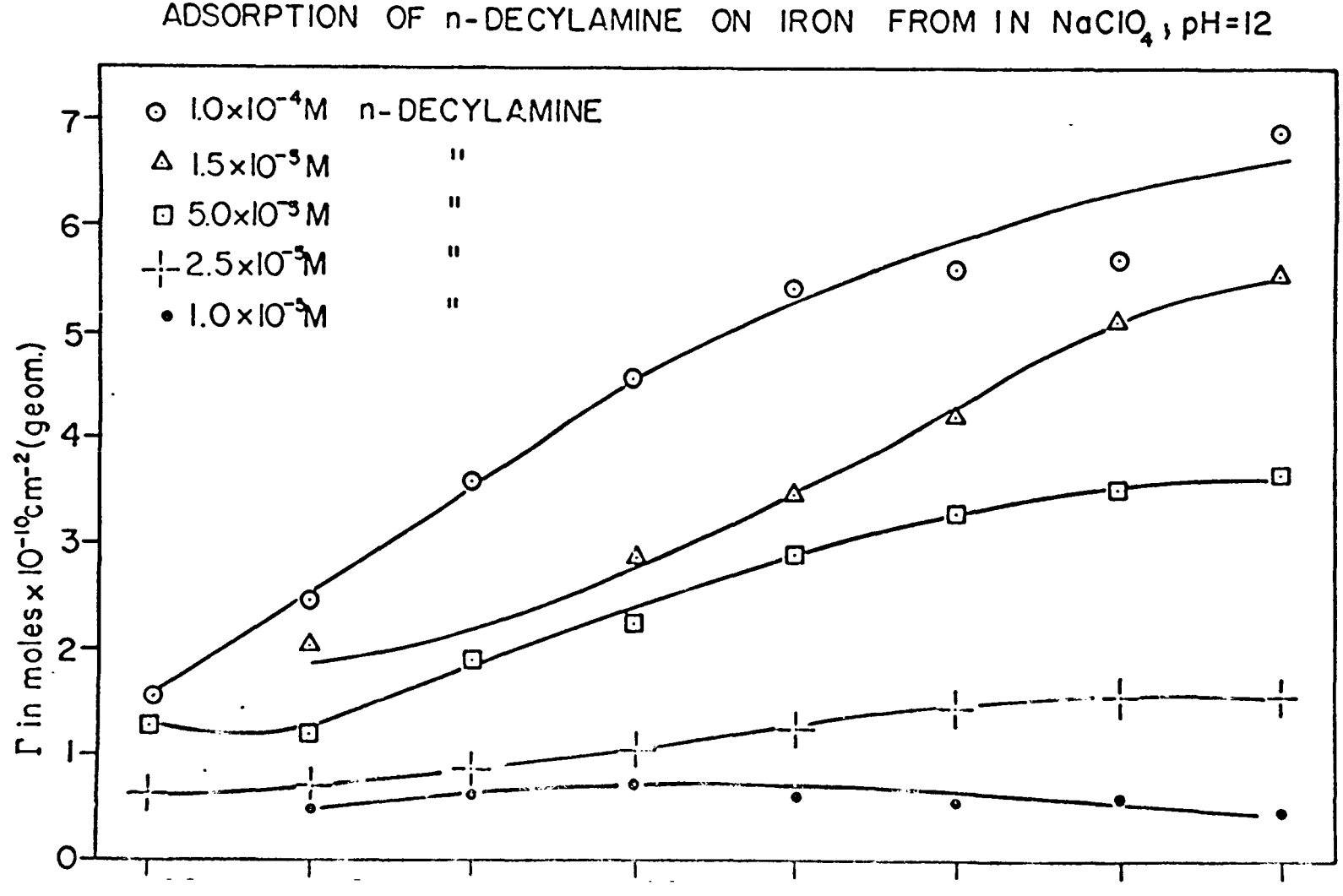
ADSORPTION OF n-DECYLAMINE ON IRON FROM IN NaClO4 , pH=12
1.0×10⁻⁴M n-DECYLAMINE
1.5×10⁻⁵M "
5.0×10⁻⁵M "
2.5×10⁻⁵M "
1.0×10⁻⁵M "
Γ in moles x 10⁻¹⁰cm⁻²(geom.)
0
1
2
3
4
5
6
7

FIG.9

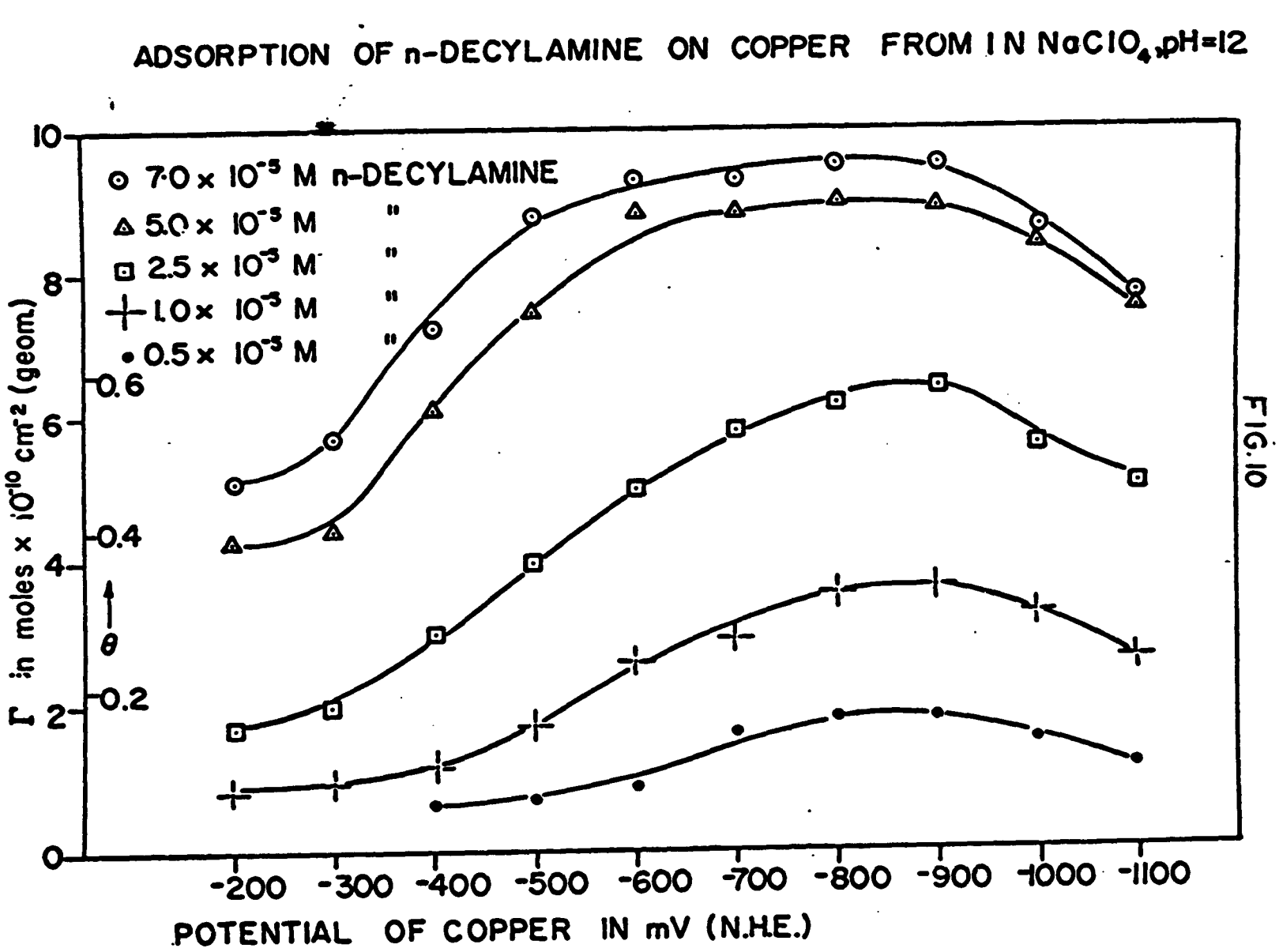
ADSORPTION OF n-DECYLAMINE ON COPPER FROM 1 N NaClO4, pH=12
7.0 x 10⁻⁵ M n-DECYLAMINE
5.0 x 10⁻⁵ M "
2.5 x 10⁻⁵ M "
1.0 x 10⁻⁵ M "
0.5 x 10⁻⁵ M "
Γ in moles x 10⁻¹⁰ cm⁻² (geom.)
θ
0
0.2
0.4
0.6
2
4
6
8
10
-200 -300 -400 -500 -600 -700 -800 -900 -1000 -1100
POTENTIAL OF COPPER IN mV (N.H.E.)

FIG. 10

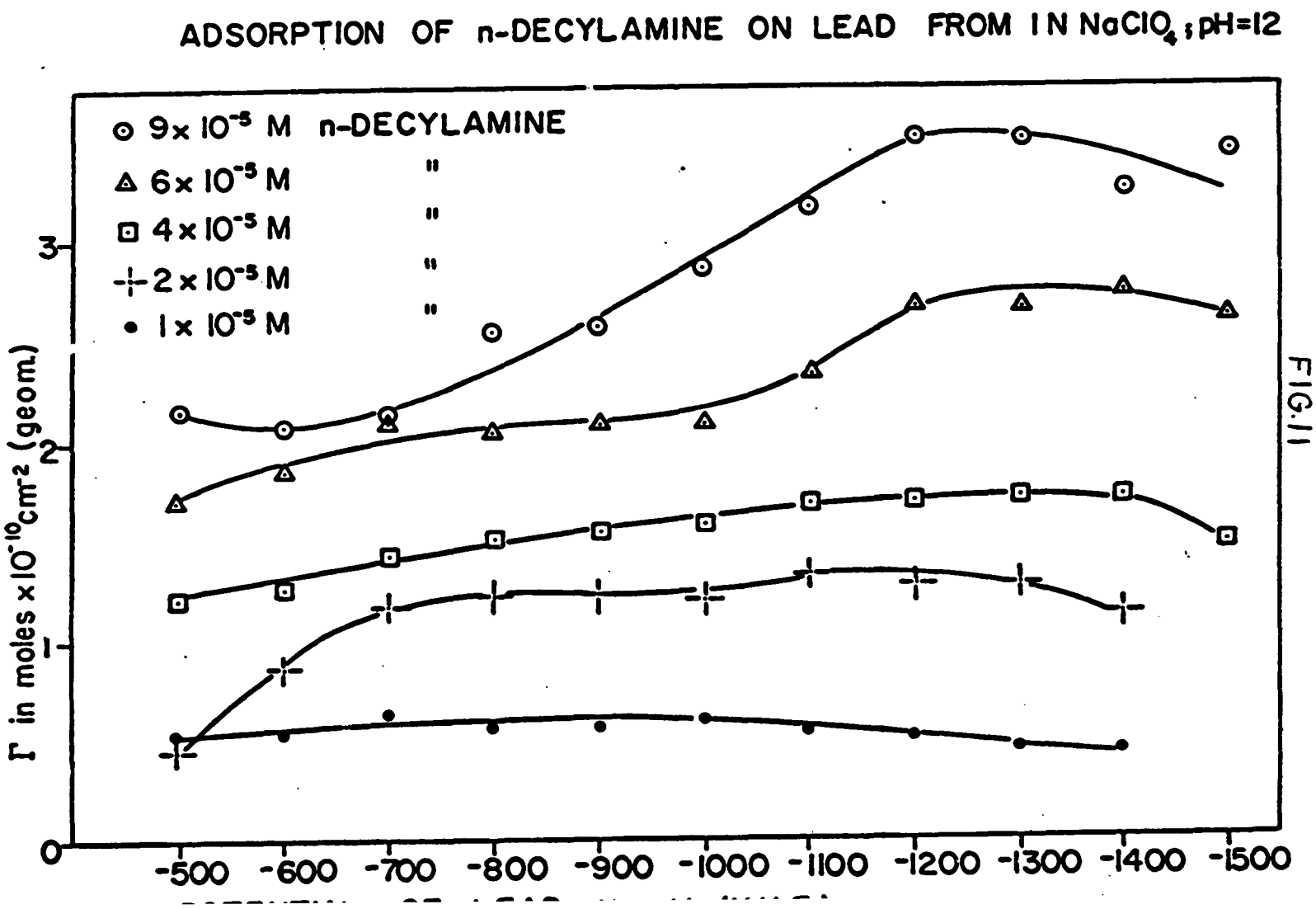
ADSORPTION OF n-DECYLAMINE ON LEAD FROM 1 N NaClO4 ; pH=12
⊙ 9x 10⁻⁵ M n-DECYLAMINE
△ 6x 10⁻⁵ M "
⊡ 4x 10⁻⁵ M "
-+- 2x 10⁻⁵ M "
• 1x 10⁻⁵ M "
Γ in moles x10⁻¹⁰cm⁻² (geom.)
0
1
2
3
-500 -600 -700 -800 -900 -1000 -1100 -1200 -1300 -1400 -1500

FIG. 11

ADSORPTION OF n-DECYLAMINE ON PLATINUM FROM IN $NaClO_4$, pH=12

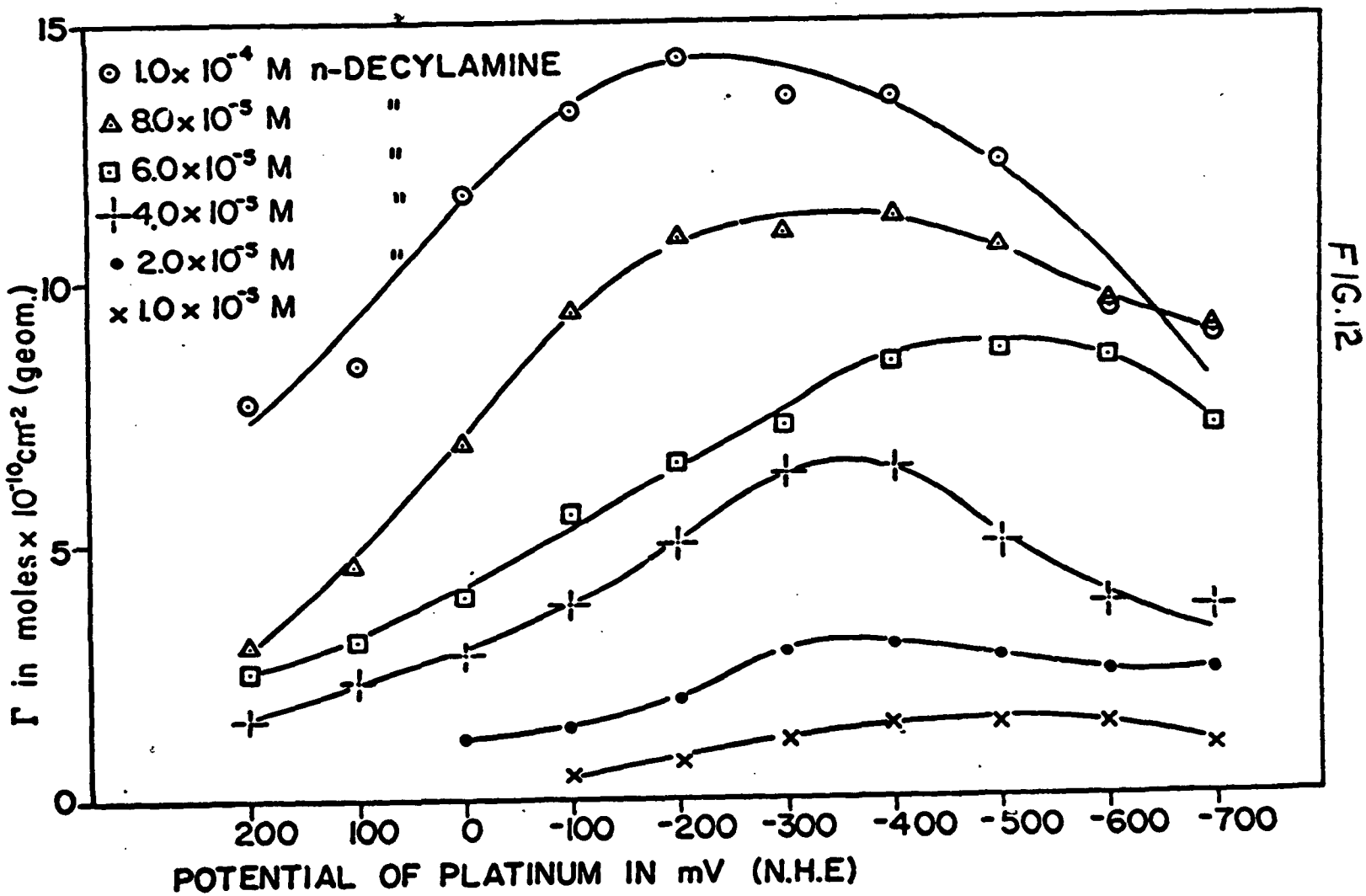

FIG. 12

NATURE OF CATALYSTS

I. Introduction

There are several modern methods of studying catalyst surfaces: 1. Ellipsometry, 2. Electron Microscopy and 3. Electron Diffraction.

1. Ellipsometry. The pioneering work of Drude (1890) and Tronstad (1931) revealed clearly that ellipsometry -- the measurement of the effect of reflection on the polarization state of light -- would constitute a powerful technique for the study of surface films, in particular, their thickness and refractive index. Apart from the fact that ellipsometry is capable of detecting extremely thin oxide films ($\sim$ 1 Å), it presented possibilities of being developed into an in situ method (i.e. measurement through a solution, hitherto an unachieved aim in the examination of electrode surfaces).

In view of the fact that the electrode surface is of crucial importance to electrode processes, attention has been devoted in this Laboratory to the problem of utilizing ellipsometry for in situ electrochemical studies of film formation and growth on mirror electrodes immersed in aqueous solutions. In such studies, two major problems arise: (a) the presence of electrolyte may be incompatible with the establishment of a film-free state of the metal surface, required as an optical reference state; (b) film growth may occur much faster than can be matched by methods normally used for analyzing elliptically polarized light. These problems have been circumvented by the use of an electronic potentiostat which has permitted the development of the following types of techniques. The basis of the use of the potentiostat is that the state of a metal-solution interface is a function of the potential difference across the interface.

2. Electron Microscopy. Many of the fundamental problems of electrode kinetics have matured to a stage where an investigation of the crystal morphology and structure of electrode surfaces is of prime importance. It has already been mentioned that continuous in situ optical microscopy (magnification $\sim$ x 500) of growing electrodeposits is being carried out in this Laboratory. In order to attain much greater resoltuion (magnification $\sim$ x 20000) in the study of electrodeposits and other surfaces, a Hitachi HS-6 Electron Microscope has recently been acquired. This microscope has been installed and commissioned. It is now in use for study of replicas of electrode surface.

3. Electron Diffraction. The Hitachi HS-6 Electron Microscope can be used for reflection electron diffraction to obtain structural information on electrode surfaces. This Laboratory has amongst its personnel members who have a background in crystallography and electron diffraction, making it possible to proceed in the immediate future with diffraction studies of surfaces.

II. Experimental

1. Qualitative Ellipsometry of Film Formation and Growth. The state of the mirror electrode surface, with respect to film formatinn and growth, is optically monitored in situ by the ellipsometer. Initial potentiostatic maintenance of a film-free optical reference state is terminated by a fast switch which almost simultaneously imposes a constant anodic current. If an induction time is required for film formation (the latter being signalled by an ellipsometer intensity "jump"), then the new technique of "chronoellipsometry" (analogous to

the electro-analytical technique of chronopotentiometry) permits the investigation of anodic processes of the dissolution-precipitation type. The mechanism of formation of calomel films on mercury pools has been extensively studied. The results have thrown new light on the calomel electrode. Preliminary work has also been done on passivating films on nickel. Initial experiments indicate that the passivating film is formed by a dissolution-precipitation mechanism. Alternatively, a simultaneous record of potential-time and ellipsometer intensity-time transients can serve to define the potential at which film growth commences. This technique has been adopted in a study of oxide formation on platinum where it has been shown that an oxide film is formed at potentials more positive than 1 V.

2. Quantitative Ellipsometry Study of Steady-State Films. The potentiostat is used to hold the potential at various values and at each value the optical components of the ellipsometer are set for extinction. The thickness and refractive index of the surface film are calculated for each potential, thus making it possible to construct thickness-potential curves. A preliminary study on platinum in acids solutions has been carried out on these lines. The detailed calculation of the thickness, refractive index and conductivity of the oxide at various potentials is in the process of computation by the University Computer Service.

MECHANISM OF ELECTRO-CATALYSIS

I. Introduction

A study of the electro-oxidation of certain systems (ethylene/sulfuric acid, acetylene/sulfuric acid) has been carried out on a number of metals (Pt, Ir, Rh, Au, Pd). In order to evaluate the role of the metal quantitatively, bright metal surfaces with a well-defined surface pretreatment have been investigated. Studies have been carried out on the overall reaction and the dependence of the reaction rate on potential, surface pretreatment, pH of the solution, oxygen coverage and the concentration in solution.

The experimental techniques used here are conventional in electrode kinetic investigations: A three compartment cell (anode, counter electrode, reference electrode) was used in connection with a special furnace to protect the metal in an inert atmosphere. The reaction products were detected and determined quantitatively utilizing a gas chromatography. Test galvanostatic studies were carried out using an oscilloscope in connection with standard photographic equipment.

The general results of this study are:

1. Current-potential: A linear relation log i vs potential (Tafel line) is obtained in all cases (Fig. 13-17). Steady state (constant current with time) is reached in a few seconds (e.g., see Fig. 13), in the potential region concerned.

2. Potential-pH: For Pt, Ir and Rh a regular shift of potential with pH of $(\frac{\partial E}{\partial pH}) = 70 - 75$ mV $= \frac{RT}{F}$ is obtained (see Fig. 15 - 17). For Au and Pd, however, a chenage of pH has no effect.

3. Current-pretreatment of metal surface: Surfaces pretreated by

heating to 1/2 of the melting point gave lower currents (1.5 to 2 times) compared to surfaces pretreated by a cycle of anodic oxidation-cathodic reduction. The mechanism of the reaction was not changed (constant Tafel slope).

4. Current reactant concentration relation: A typical dependence is plotted in Fig. 18 and Fig. 19. The mechanism of the reaction was not affected (constant Tafel slope).

5. Current-oxygen coverage: Oxygen coverages of all metals vs potential are plotted in Figure 20. By comparing the oxygen coverages with the Tafel slopes (Fig. 13 - 17) it can be seen that already low oxygen coverages of about 0.1 show a pronounced effect on the Tafel lines by blocking parts of the active surface.

6. The overall reaction and reaction rates: The metals can be separated into two groups according to their catalytic activity (Table 1).

TABLE 1

REACTION PRODUCTS AND ELECTRODE KINETIC DATA IN ELECTRO-CATALYSTS OF HYDROCARBON OXIDATION

	Reaction Product		pH dependence $(\frac{\partial E}{\partial pH})_i$	Tafel Slope $(\frac{\partial E}{2.3\,\partial \log i})_{pH}$
Group I	Pt	CO_2	70	160
	Ir	CO_2	75	132
	Rh	CO_2	70	155
Group II	Pd	Aldehydes, ketone	0	72
	Au	" "	0	110

It can be seen that the metals converting the fuel to CO_2 show a similar dependence on pH and give Tafel slopes of 2RT/F.

The influence of electronic factors (electronic work function, d-band vacancies) and geometric factors (lattice parameters) on the oxidation rate has been evaluated. A close relation between the reversibility of the oxide formation and the reaction sequence could be shown.

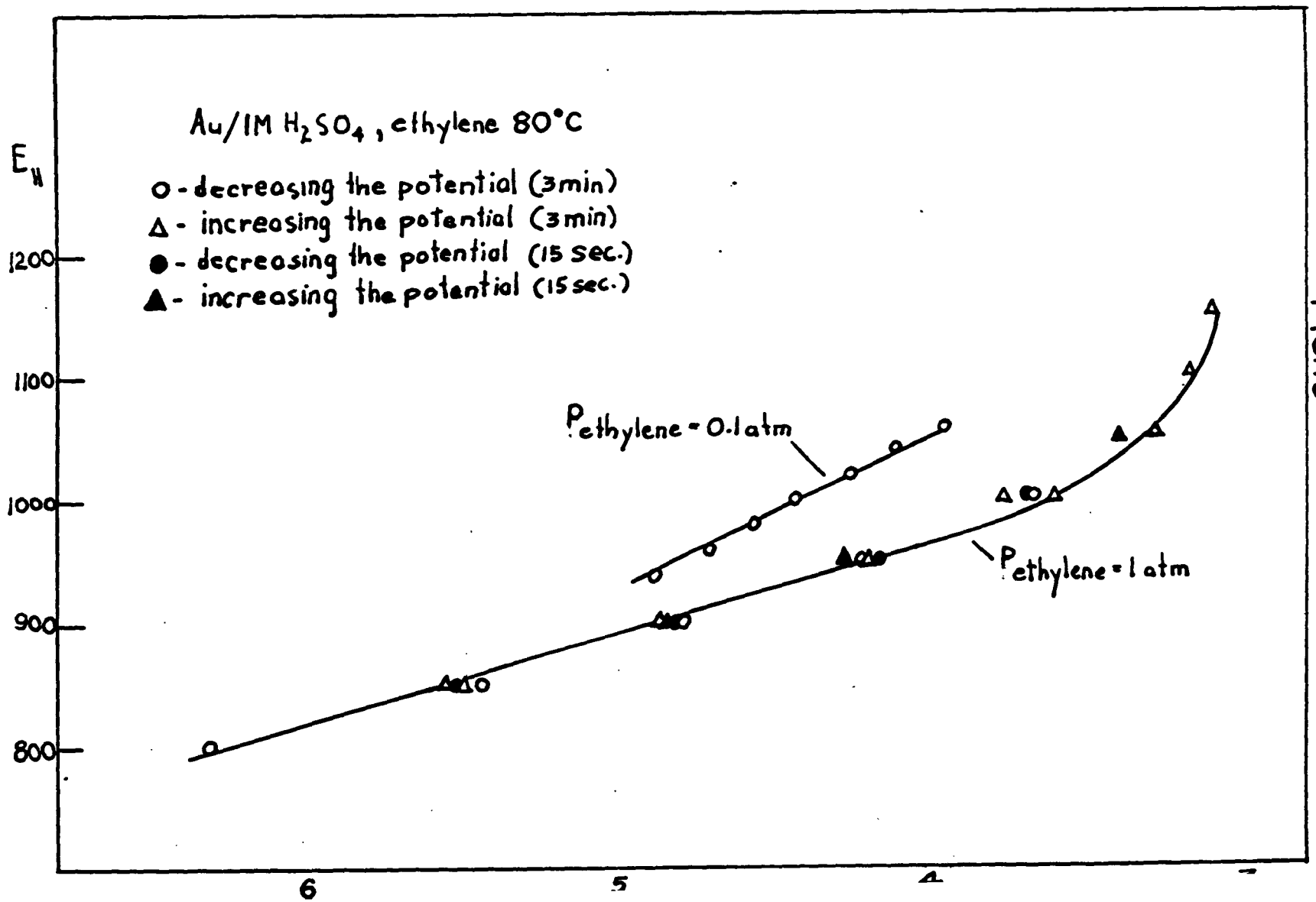
Au/1M H_2SO_4, ethylene 80°C
E_H
o - decreasing the potential (3min)
Δ - increasing the potential (3min)
● - decreasing the potential (15 sec.)
▲ - increasing the potential (15 sec.)
1200
1100
1000
900
800
$P_{ethylene}$ = 0.1 atm
$P_{ethylene}$ = 1 atm
6
5
4

FIG. 13

FIG. 14

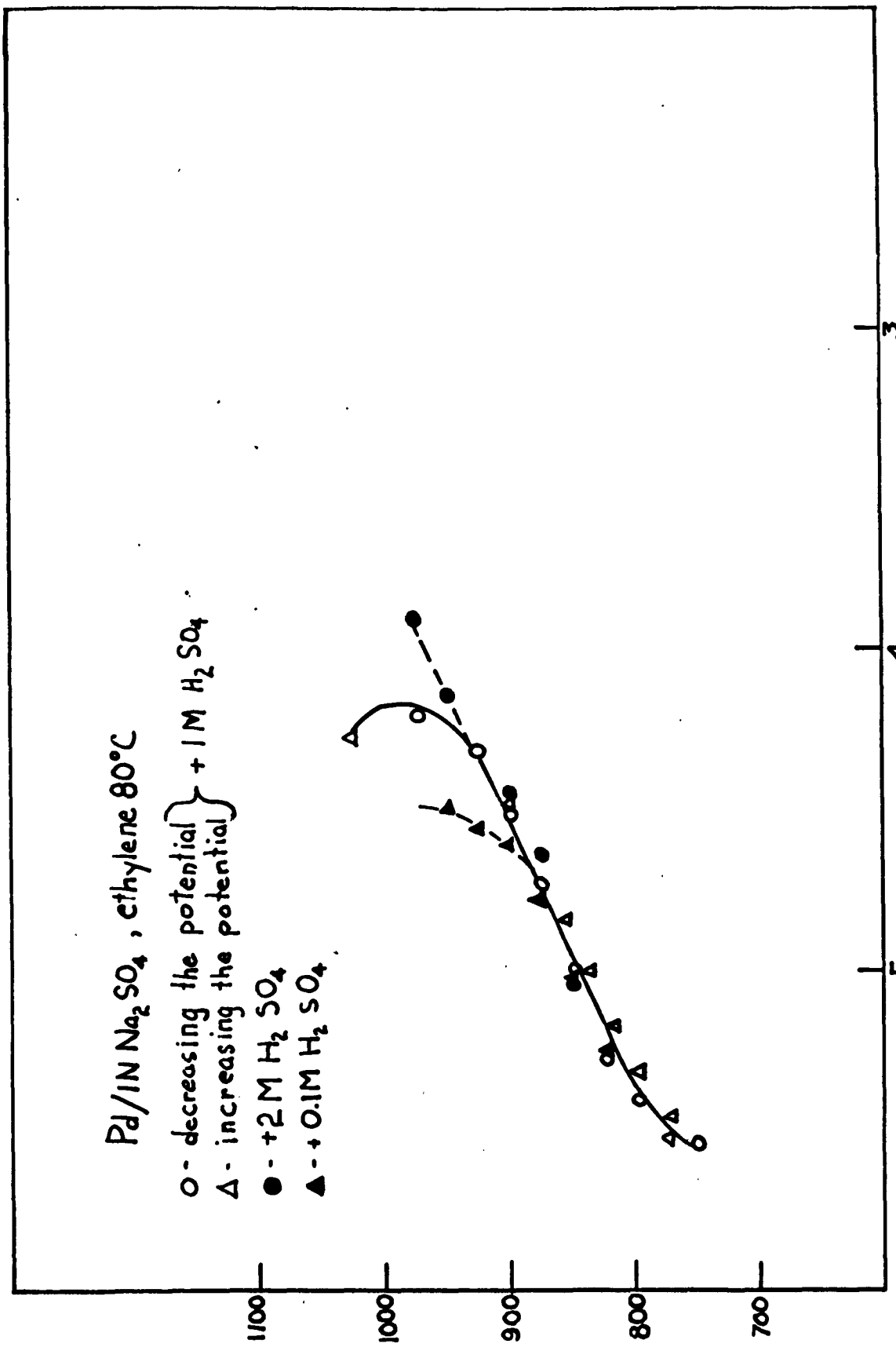
Pd/1N Na2 SO4 , ethylene 80°C
O - decreasing the potential } + 1M H2 SO4
Δ - increasing the potential
● - +2M H2 SO4
▲ - +0.1M H2 SO4
1100
1000
900
800
700
3
4
5

FIG 15

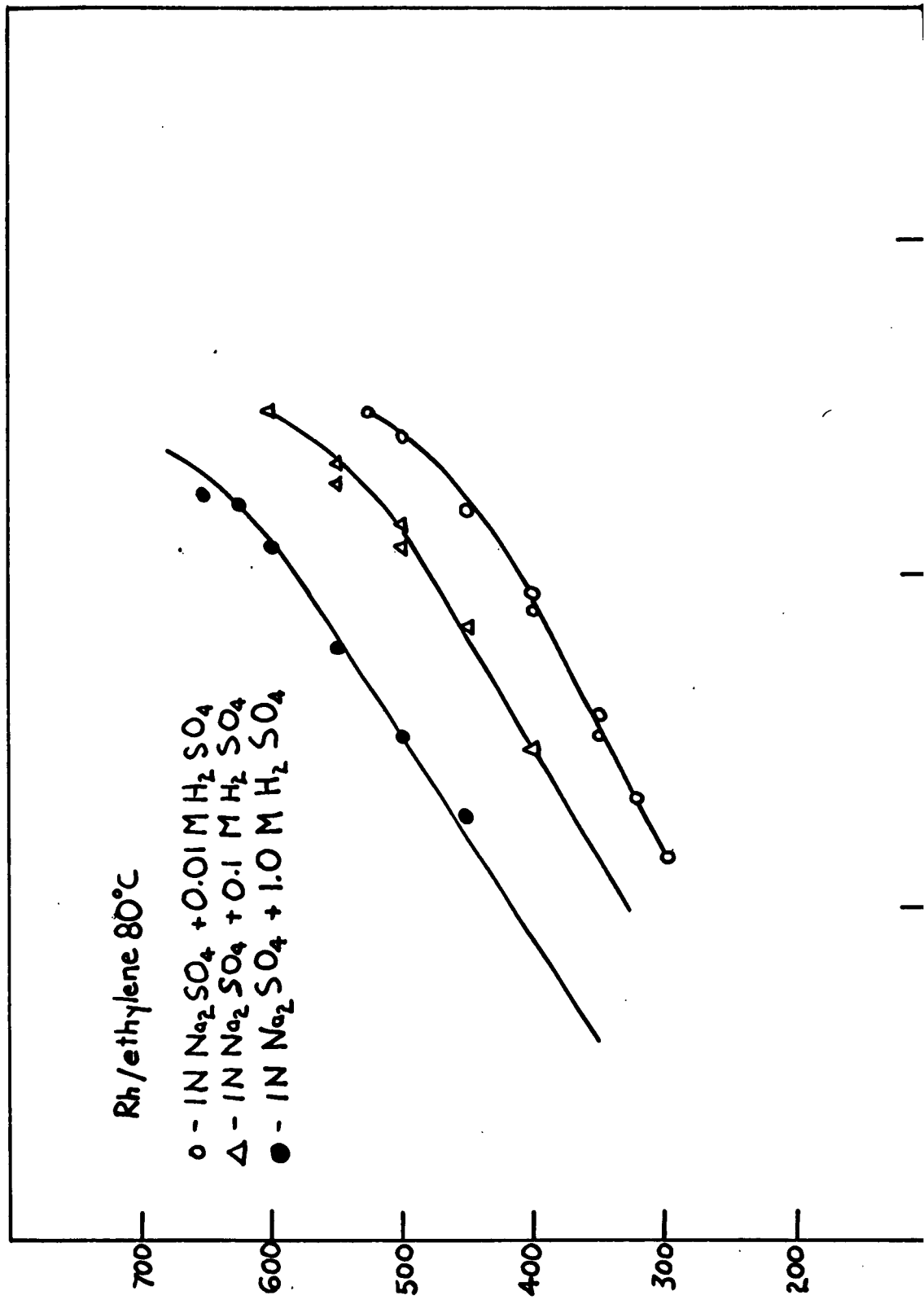
Rh/ethylene 80°C
o - 1N Na2SO4 + 0.01 M H2SO4
Δ - 1N Na2SO4 + 0.1 M H2SO4
● - 1N Na2SO4 + 1.0 M H2SO4
700
600
500
400
300
200

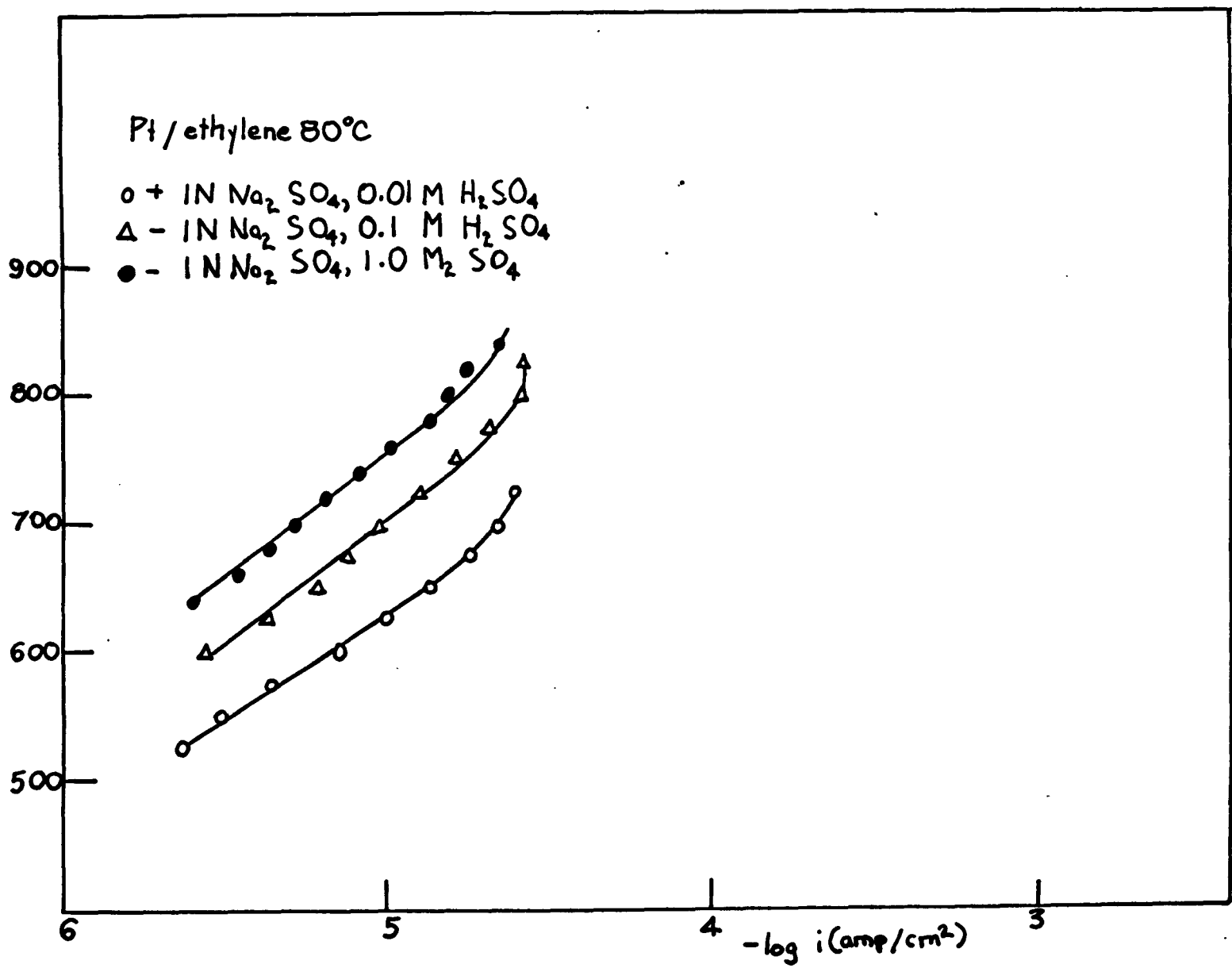
Pt / ethylene 80°C
o + 1N Na2 SO4, 0.01 M H2SO4
Δ - 1N Na2 SO4, 0.1 M H2 SO4
● - 1 N Na2 SO4, 1.0 M2 SO4
900
800
700
600
500
6
5
4
3
-log i (amp/cm2)

FIG. 16

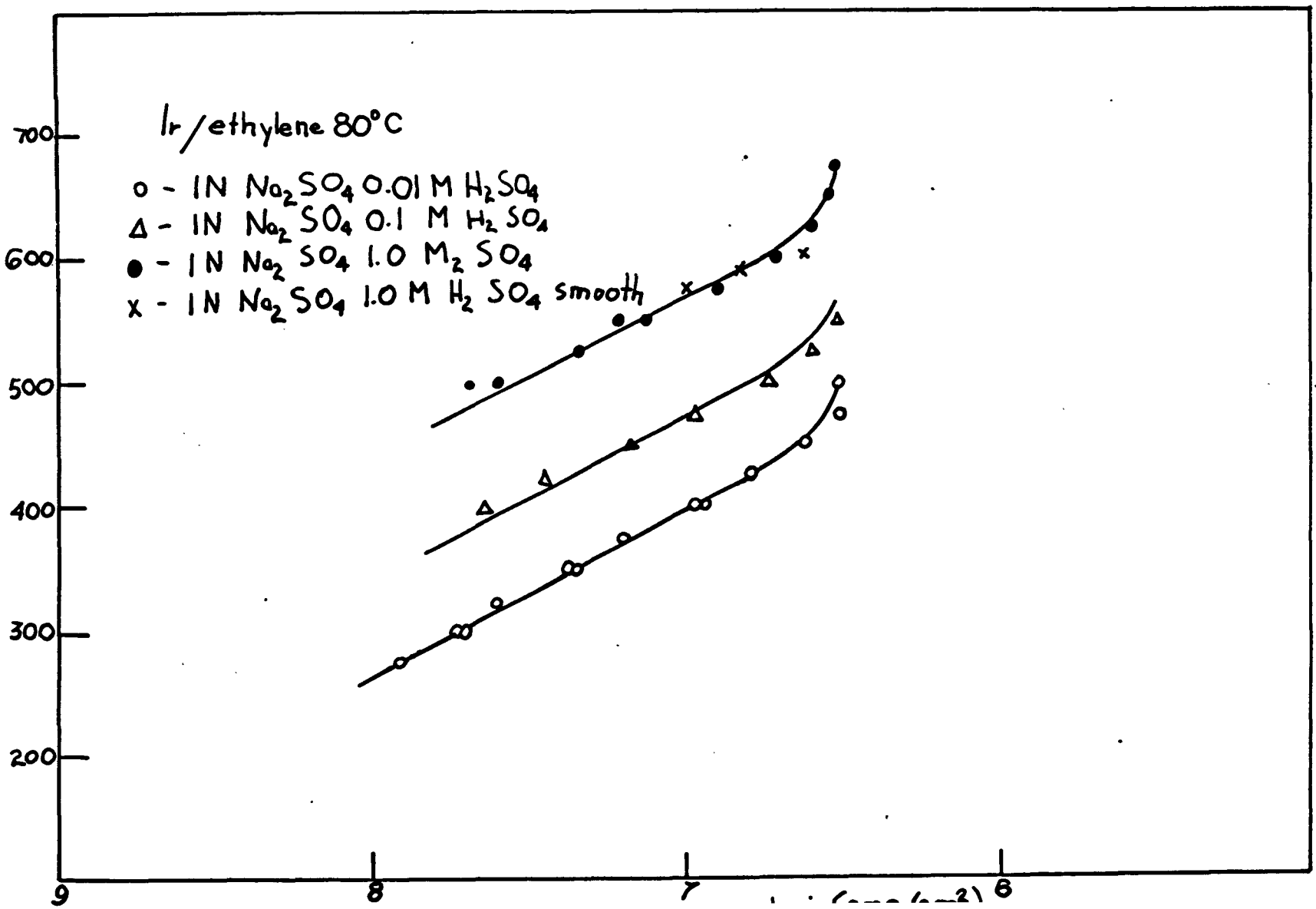
Ir/ethylene 80°C
o - 1N Na2SO4 0.01 M H2SO4
Δ - 1N Na2SO4 0.1 M H2SO4
● - 1N Na2SO4 1.0 M2SO4
x - 1N Na2SO4 1.0 M H2SO4 smooth
700
600
500
400
300
200
9
8
7
6

FIG. 17

FIG. 18

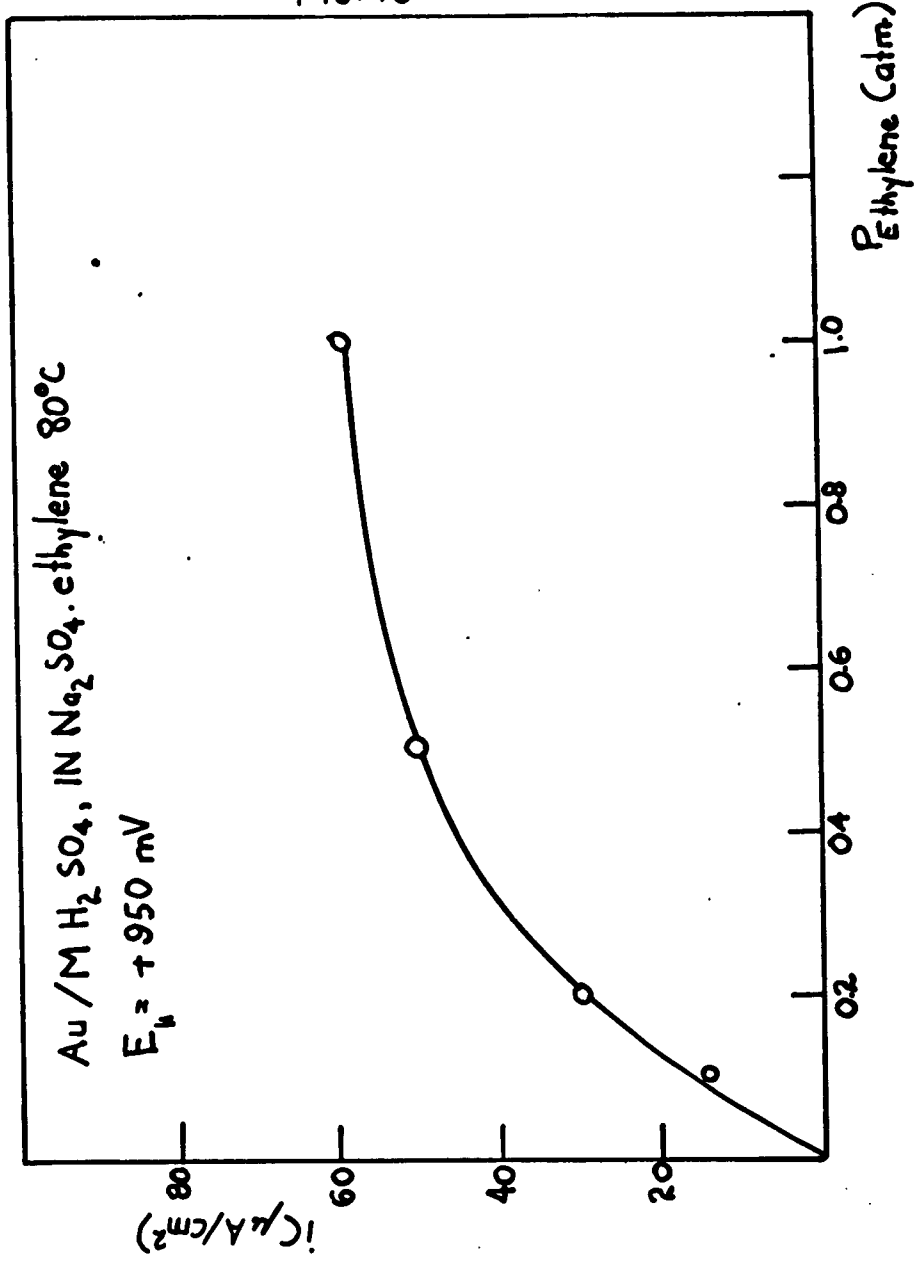
Au /M H_2SO_4, IN Na_2SO_4. ethylene 80°C
E_h = +950 mV
i(μA/cm²)
20
40
60
80
0.2
0.4
0.6
0.8
1.0
$P_{Ethylene}$ (atm)

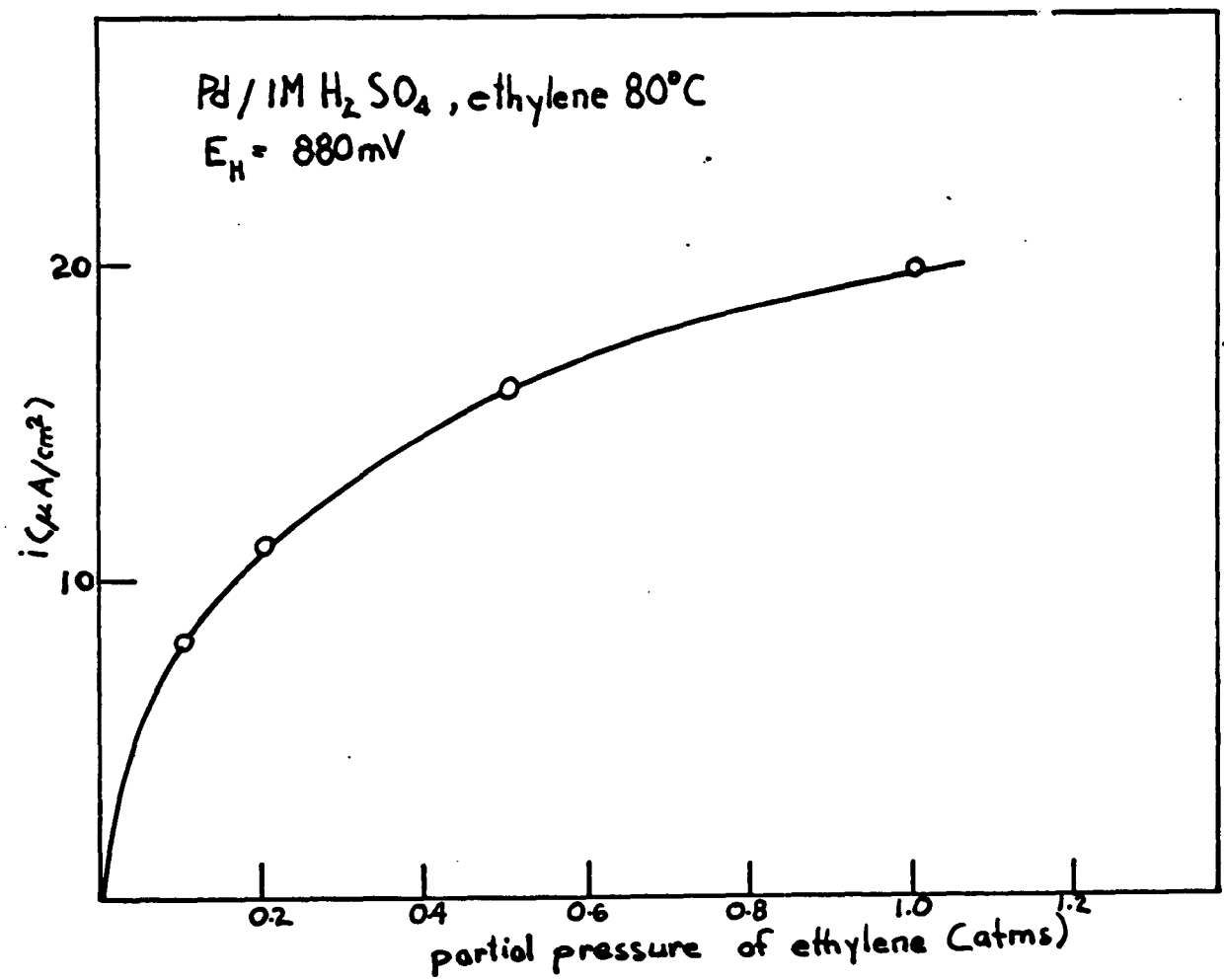
Pd / 1M H_2SO_4 , ethylene 80°C
E_H = 880mV
20
10
$i(\mu A/cm^2)$
0·2
0·4
0·6
0·8
1·0
1·2
partial pressure of ethylene (atms)

FIG. 19

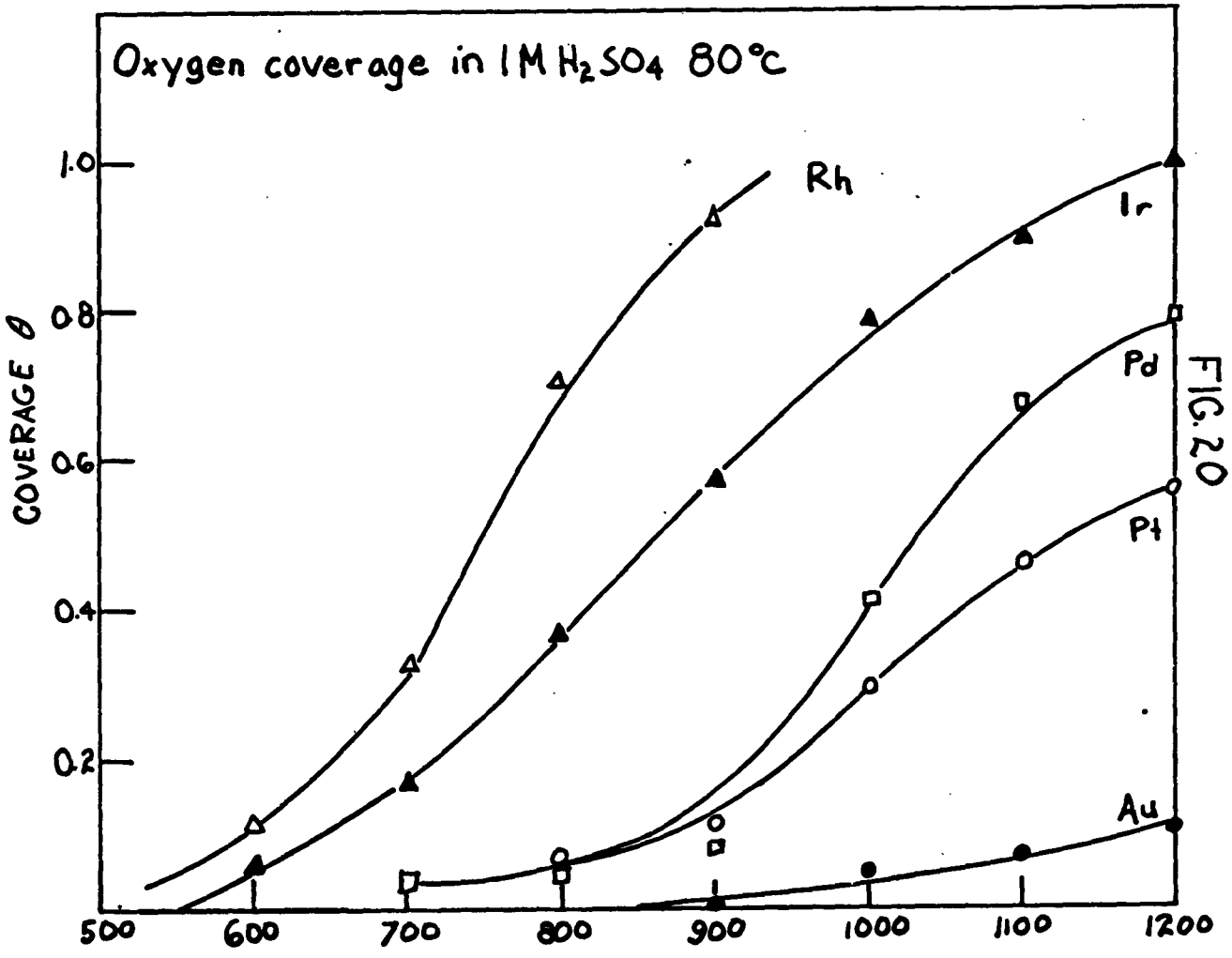
Oxygen coverage in 1M H_2SO_4 80°C
COVERAGE θ
1.0
0.8
0.6
0.4
0.2
500
600
700
800
900
1000
1100
1200
Rh
Ir
Pd
Pt
Au

FIG. 20

STUDIES OF THE MECHANISM OF POROUS ELECTRODES

I. Introduction

Recent progress has been made in elucidating the specific modes of interaction and current control for thin layers of electrolytes on platinum electrodes. The equivalence of such models for actual porous-electrode fuel cell systems is well known. In particular, the work of Will[4] has shown that the major amount of current passing through a meniscus region is actually concentrated over an area associated with neither the very thin film nor the bulk solution but an intermediate region. The actual current density in this region is relatively high, e.g., $\approx$ 30 mA/cm^2, and is controlled by diffusion of hydrogen which enters the electrolyte from the gas phase and passes through the thin film and by the lateral resistance of the integrated path along the working electrode through the solution in the meniscus region. In other words, the permissible current results as a net balance between the dissipative effect of solution resistance and path length for hydrogen permeation. It is clear that a low resistance path also provides a very long diffusion path and vice versa for the meniscus model of Will[4] and generally for any geometry in which the direction of flow of current is perpendicular (or at least has a net resolved component in the perpendicular direction) to the direction of flow of species involved in the electrode reaction.

The partially immersed (meniscus) electrode studied by Will[4] is a suitable model for processes occurring in the "larger" pores of a practical porous electrode. However, the localization of current demonstrated by Will for even large equivalent pores raises the important question as to the magnitude of actual current-sharing by the very small

pores in an actual porous-electrode system. (N.B. The work of Will has demonstrated not only the efficacy of thin film current control but has also cast doubt on previous proposals made by Justi et al[6] for a three phase local intersection control based on a slow step due to hydrogen diffusion on the unwetted electrode area).

II. Present Approach

In order to elucidate the nature of current control in very small pores, an equivalent model has been devised which is both amenable to theoretical calculation and also offers a distinct possibility for practical experimental control of the several variables of importance. In particular, it was noted that the model used by Will becomes non-applicable in the limit as equivalent pore diameter decreases. Analysis of Will's proposed theoretical basis shows that his treatment begins to break down for pores with diameters less than 50 microns and becomes inapplicable for pores which have diameters less than 5 microns. These conclusions are evident from consideration of the nature of the assumptions utilized by Will in order to arrive at even a first approximation to the complex mathematics of the situation.

Rather than prepare complex analytical evaluations of models resembling that of Will, it was considered more instructive to adopt a geometry which was more readily translatable in terms of micro-pores and which also permitted meaningful mathematical analysis with a minimum of assumptions.

The present model may be described as a fissure electrode in which a narrow gap is introduced between a working planar electrode and

axis of symmetry represented by a non-conducting plane. Gas is introduced at the top of the slit and electrolyte joins a large reservoir at the bottom. The reservoir compartment contains the counter-electrode and the reference electrode. The reservoir itself is a controllable volume so that height of electrolyte in the slit can be controlled to any desired value to within 0.1 mm. This arrangement has been chosen for the following reasons:

1. Diffusion of reacting species may be considered as purely one-dimensional, i.e. down the slit, especially for equivalent narrow pores.

2. The easiest surface to control to extremely close size tolerances is an optical flat.

3. Spacing can be varied at will with a flat geometry so that a wide range of equivalent pore sizes (.003 mm - 1 mm) may be controllably reproduced.

4. Uniformity of pore corresponds to precision of alignment in the present model; this is feasible with careful machine techniques to an angular misalignment between flats of less than 1 minute of arc.

5. With controllable non-parallelism introduced, concentration changes in the electrolyte within the pore may be studied by shifts in the interference fringes which may be viewed simultaneously with the procedure of the experiment. (Optical manipulation is possible because of the transparent window leading to the working compartment, i.e. the slit region). (see Fig. 1).

6. With large spacing in the slit the model reduces to the equivalent case treated by Will[4] so that a direct check of results will be possible.

The construction of the cell is shown in Fig. 1. The body of the cell (A) is a block of "Teflon" 4" x 4" x 2" with a cylindrical hole 2" in diameter through its center. A close-fitting piston (B) of "Teflon" sealed with a Viton "A" O-ring serves as the mount for the working electrode (C). This electrode is a block of glass, precision ground to a tolerance of 1/4 light fringe. A thin ($\approx 1\mu$) film of platinum is evaporated and/or sputtered on the surface to serve as the electrode. A three axis micro-manipulator (not shown) controls the alignment and spacing of this electrode relative to the clear fused silica face-plate (D), which is face sealed to the "Teflon" block with a "Viton A" O-ring (E). In the electrolyte reservoir, (F) is the palladium tube counter electrode (G). This tube (6 mm O.D. x 0.12 mm wall) has a platinum wire and electrolyte inside it, forming a local cell which scavenges dissolved H_2 from the solution, and prevents bubble formation in the reservoir compartment. The electrolyte inside the tube is circulated through a constant temperature bath, and serves as a heat exchanger for maintaining constant temperature in the cell proper. Volume changes in the reservoir are controlled with a modified Gilmont micro-burette (not shown) which is connected to the cell with a "Teflon" fitting (H) similar to the "Swagelok" design for metals. Connections to the hydrogen gas compartment (J) are made in similar fashion.

III. Instrumentation

The following instrumental arrangements are possible.

1. Controlled potential of the working electrode utilizing the reference electrode together with a high-precision potentiostat.

2. Current is monitored with an electrometer input-recorder arrangement and/or oscilloscope. Steady-state and transient currents will be evaluated in terms of gap spacing and electrode treatment. The pretreatment will be varied so as to cover a wide range of electrode surface preparation and catalyst additions. However, preliminary experiments will be concerned with the platinized platinum electrode with hydrogen dissolving in 1 N H_2SO_4.

References

4. F. Will, J. Electrochem. Soc., V 110, p. 145 (1963); ibid., V 110, p. 152 (1963).

5. E. Justi, M. Pilkuhn, W. Scheibe, A. Winsel, Verlag d. Akademie d. Wissenschaften n.d. Literatur. Wiesbaden, 1959.

FIG. 21

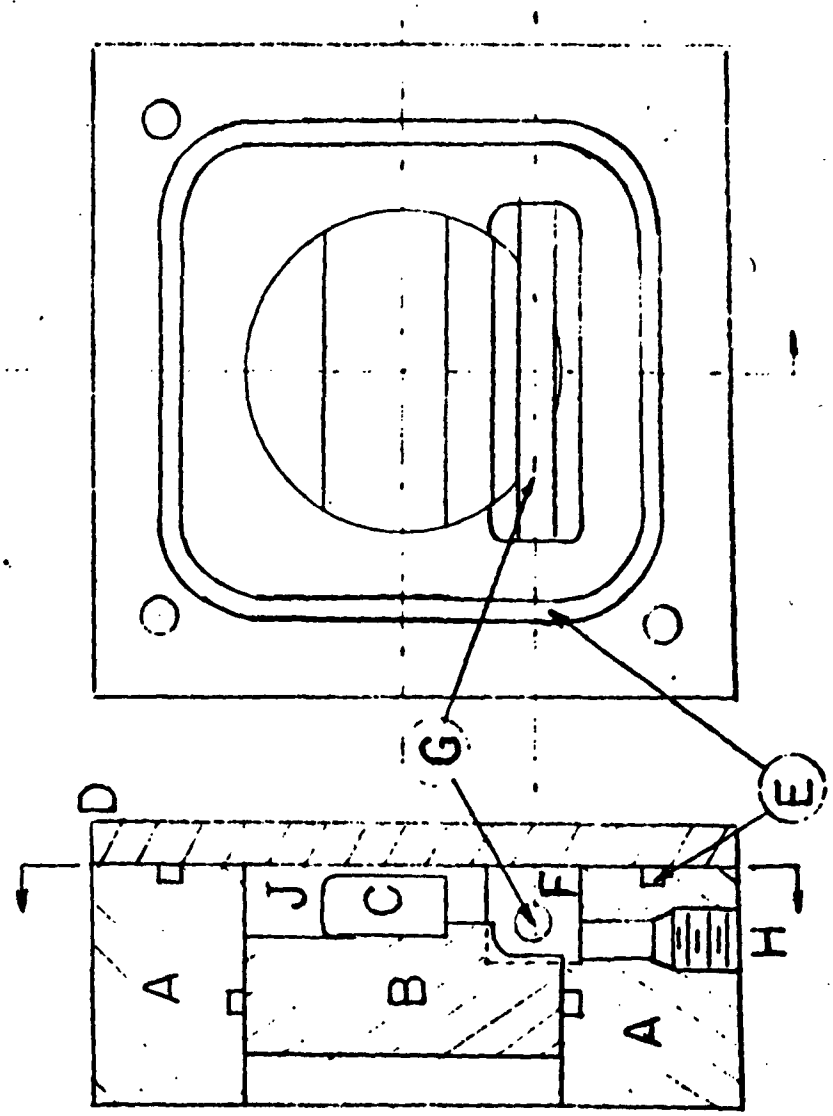

THEORY OF ELECTRIC DOUBLE LAYERS

I. Introduction

The quantity of adsorbed charge exceeding that predicted by diffuse layer or "Gouy" theory is better known as charge specifically or, more descriptively, "superequivalently" adsorbed. Since superequivalently adsorbed ions are so instrumental in affecting electrode potentials and kinetics of charge transfer reactions, it is deemed worthwhile to study the nature of the binding forces involved.

Previous views, largely due to Grahame,[6] have largely been that ions are held to the electrode surface by covalent bonds, although non-covalent binding has been suggested[7] without support. The former view was linked with the fact that the common cations (e.g., Na^+, Mg^{++}, Al^{3+}) are not superequivalently adsorbed. This linking is natural since the first ionization potential of positive ions is much greater than that of negative ions. Other evidence offered for covalent bonding is that the tendency of anions specifically to adsorb follows the same order as that of forming insoluble salts with mercury and complex ions with mercury (cf. HgX_3^-, $HgX_4^=$). When this argument is analyzed, it is found that hydration forces of the anions with water determine the latter trends, and that the strengths of the largely covalent bonds as well as the standard free energies of complex ions favor the opposite trend to that found.

The present recognition that several cations are specifically adsorbed is hard to rationalize with covalent bonds, and several qualitative arguments, regarding the nature of bonding, surface coverage and rate of adsorption, support non-covalent bonding.

Therefore, the task of this work is to examine whether available facts on superequivalent (SE) adsorption can be made consistent with a non-covalent model.

The system chosen is mercury in aqueous ionic solutions, the only system for which even a nominal amount of quantitative data exists.

II. Phenomenology of Superequivalent Adsorption

The facts to be explained are:

1. Metal charge: The quantity of ions adsorbed increases as the electrode charge opposes that of the ions. A central fact to be interpreted is that negative ions adsorb on negatively charged surfaces.

2. Ion type and size: Most cations do not adsorb measurably (i.e. group IA, IIA, Al^{+3} and transition metals which have been investigated). The large tetra alkyl ammonium ions do so considerably: Tl^{+} and Cs^{+} probably do. In the case of monovalent ions, as in the case of positive ions investigated, SE adsorption increases with an increase in ionic size (see Table II, Columns 1 and 2). Not enough divalent anions have been studied with which to establish data.

3. Se adsorption of ions is a function of the type of hydration. It appears that ions with more waters of primary hydration are the least superequivalently adsorbed (see Table II, column 3).

4. Concentration of adsorbate: The coneentration of adsorbed ions increases with bulk concentration in a manner describing familiar isotherms (i.e. a sharp rise followed by leveling out of adsorbed charge with an increase in bulk concentration.

5. Temperature: Only one paper exists: Parsons[8] obtains

TABLE II

SE ADSORPTION (IN MICRO COUL PER cm^2) FROM 0.1 m AQUEOUS SOLUTIONS AT ecm

Ion	Specific Adsorption	No.of H_2O's of Primary Hydration	Ion	Sp. Ads.	No. of primary waters of hydration
Li^+	0	5	F^-	0	4
Na^+	0	4 - 5	Cl^-	1.7	1 - 2
K^+	0	3 - 4	Br^-	5.2	1
Cs^+	0 - 0.1	1	I^-	10.6	0 - 1
Mg^{+2}	0	12	CNS^-	5	0 - 1
Ca^{+2}	0	9	NO_3^-	2.3	1
Al^{+3}	0	20	OH^-	0.1	6
$N(Me)_4^+$	7.6		CNO^-	2	
$N(Et)_4^+$	14.8				
$N(n\text{-}Pr)_4^+$	17.4				

$\Delta H \simeq$ - 12 kcal for adsorption of I^- from 1.0 m KI onto Hg at zero coverages. His entropy change (at the ecm) onto the electrode at given coverage (about 20 coul/cm^2) is - 10 e.u. per mole.

III. Model

A model was produced with which to calculate ΔH and ΔS of Se adsorption without involving covalent bonds. The model was applied to the ions F^-, Cl^-, Br^-, I^-, Na^+, K^+, and Cs^+ which produce enough

criterion to judge the model: i.e. (1) the correct order of adsorption by the ions should be followed, (2) a distinction between superequivalently adsorbing and non-adsorbing ions should result, and (3) the magnitude of ΔH_{ads} and ΔS_{ads} should be of the same order as Parsons' for iodide.

The model for ΔH included the following interactions:

(a) n H_2O molecules of adsorbed water must be desorbed from the mercury surface, leaving a space for the ion.

(b) The ion-solvent interactions are broken; this includes the ion-primary water dipole interactions and the Born energy.

(c) The ion is transported to the electrode surface where: (1) The ion interacts with the metal with image, dispersion and electron-overlap repulsion energy; (2) The ion interacts with the nearest water molecules around it causing some to orient differently than previously. This produces a gain in ion-dipole interaction energy, a structure (H-bond) breaking in some water molecules, and a partial desorption of some neighboring, adsorbed waters: (3) The ion Born charges the new environment.

(d) The hole left by the ion in solution fills with water molecules with a gain in energy due to H bond formation.

The overall heat of specific adsorption is given by

$$\Delta H_{S.E.ads} = \sum_{x=a}^{d} \Delta H_x. \qquad (1)$$

The exact model for obtaining the enthalpy terms in (1) is found in a paper soon to be submitted. The essentials are: (i) n_2 water molecules surround an ion in solution, with one H bond to the solution broken in each case; (ii) n_1 of these waters are primary, or experience maximum

ion-dipole interaction energy; (iii) the electrode is covered with water molecules to the fraction θ_w' (where $\theta_w' = 1$ is maximum possible coverage -- i.e. hexangonal closest packing in two dimensions); (iv) the adsorbed water molecules experience dispersion, image and repulsion energy with the electrode, H-bonding energy (two per molecule) with the bulk solution and lateral repulsion energy; (v) the adsorbed ion is surrounded by n_2' water molecules of which n_1' are primary; (vi) the distance of a given ion (center) from the surface is r_i, and the fraction of the ion surface blocked (to hydration) by the electrode is F.

The terms in (i) to (vi) were obtained or calculated: r_i was found by minimizing the interaction energy (dispersion + image + repulsion) between the ion and metal. Repulsion constants were obtained from alkali halide crystals of like ions. θ_w' was obtained from gas phase (water) adsorption data, thermodynamic data and a repulsion calculation.

$$n_2 = \frac{(r_i + r_w)^2}{r_w^2} \qquad \text{where} \qquad \left(\frac{V_{molar}}{N}\right)_{H_2O} = 0.6.$$

n_1 was obtained from experimental and theoretical values in the literature. $n_1' = (1 - F)\, n_1$ and $n_2' = (1 - f)\, n_2\, (1 - F) + f\, \theta_w'\, n_2\, (1 - F)$ where f is the fraction of primary waters surrounding an adsorbed ion which also touch the electrode surface.

The results, based on the model, are shown in Table III for the ions selected.

IV. Results

A calculation of the entropy of specific adsorption can be made by considering the following changes: (i) an ion, in being adsorbed,

TABLE III

Ion	Na^+	K^+	Cs^+	F^-	Cl^-	Br^-	I^-
$\Delta H_{SE\ ads}$ (kcal/mole)	+5	-2	-12	+4	-14	-15	-16

loses 1 degree of hindered translation and gains 1 degree of vibration. From the ion-metal interaction S_{vib} is found, and knowing the free volume of the solution and free area of the electrode permits the first calculation. (ii) The n desorbed water molecules gain entropy, found from the thermodynamic data mentioned earlier. (iii) The non-primary water molecules formerly surrounding the ion in solution lose entropy since they acquire more hydrogen bonds, and the primary water molecules which formerly surrounded the ion have their motions modified. (iv) The reverse process to (iii) occurs with the water molecules neighboring the ion at the electrode. (v) The Born entropy change is found to be negligible.

The entropy calculations, although still needing refining, indicate that the entropy change accompanying specific adsorption onto surfaces with ion coverages of a few microcoulombs per cm^2 (that for the larger halide ions) is the order of 0 to - 10 e.u./mole.

Hence the free energy of superequivalent adsorption is a few kcal (up to 3) more positive than the enthalpies shown in Table II.

V. Discussion of Results

Considering an isotherm for relating the amount of specific adsorption to the free energy of specific adsorption,

$$n_{i,ads} = n_{i,soln} K e^{-\beta F/RT}$$

we can say the following concerning the results:

(1) The order of specific adsorption follows favorably that given in Table II, for the various ions. (2) The positive value for $\triangle F$ in the case of Na^+, F^- and K^+ tendsto disfavor specific adsorption. (3) The value for $\triangle H_{SE\ ads}$ for I^- compares favorably with Parsons' experimental value (which has several kcal doubt, as to its actual value). (4) The free energy difference is small among the three larger halides and Cs^+. A rather wide variety of reasonable changes in the model still produces the order shown along with rather small differences. That the free energy difference between I^-, Br^- and Cl^- is indeed small (within 0 - 2 kcal) is shown by substituting experimental values of $n_{i,ads}$ into the isotherm and solving for F, with reasonable values chosen for K. Cs^+ appears to be adsorbed too much from the relative $\triangle F$ value. However, it must be remembered that q_{SE} has never actually been measured for Cs^+, but only estimated from capacity curves.

References

6. Grahame; Chem. Rev. 41, 441 (1947).
   Grahame and Soderberg, J. Chem. Phys., 22, 449 (1954).
   Grahame, J. Electrochem. Soc., 98, 344 (1951).
7. Bell, Levine and Calvert, Can. J. Chem. 40, 518 (1962).
   Gellings, J. Appl. Chem. 12, 113 (1962).
8. Anderson and Parsons, 2nd Int. Congress of Surface Activity III, Butterworths, London.